GAMMA-RAY STUDIES OF ^{71}Ge

By

DAVID THOMAS KELLY, M.Sc.

A Thesis

Submitted to the Faculty of Graduate Studies

in Partial Fulfilment of the Requirements

for the Degree

Doctor of Philosophy.

McMaster University

September, 1975

GAMMA-RAY STUDIES OF ^{71}Ge

DOCTOR OF PHILOSOPHY   McMASTER UNIVERSITY
    (Physics)   Hamilton, Ontario.

TITLE: Gamma-ray Studies of ^{71}Ge.

AUTHOR: David Thomas Kelly, B.Sc. (Hons)(Melbourne)

                                  M.Sc. (Melbourne)

SUPERVISOR: Professor J.A. Kuehner

NUMBER OF PAGES: x , 127.

ABSTRACT

The $^{68}Zn(\alpha,n\gamma)^{71}Ge$ reaction has been used to study the gamma decays of levels below 1.3MeV excitation in ^{71}Ge. Gamma-ray angular distributions and angular correlations of gamma-gamma cascades were measured, using Ge(Li) detectors. The results were analysed using the Compound Nucleus Statistical Reaction Model, to determine the angular momenta of most of the levels known in ^{71}Ge below 1.3MeV, and the multipole mixing ratios of their gamma decays.

The deduced level scheme has been compared with the predictions of a nuclear model calculation, in which the odd neutron in ^{71}Ge is coupled to the collective quadrupole vibrations of the ^{70}Ge core. The model allowed for a pairing residual interaction between the core neutrons, and anharmonic terms in the core vibrations.

ACKNOWLEDGEMENTS

TABLE OF CONTENTS

TABLE OF CONTENTS (CONT'D)

LIST OF FIGURES

LIST OF FIGURES (CONT'D)

LIST OF TABLES

x

CHAPTER I

MOTIVATION

The properties of nuclei in the mass region of ^{71}Ge have not, in general, been satisfactorily described by theoretical nuclear models as yet. Shell model calculations have not been reported because of the large number of particles and available states that would have to be included in a realistic calculation. The evidence for rotational structure in the nuclear levels in this region is not strong, though an explanation of some of the properties of the ^{70}Ge and ^{72}Ge nuclei has been attempted in terms of a permanent deformation of these nuclei (Kregar and Mihailovic, 1967), suggesting that the low lying states of ^{71}Ge could be derived from the motion of a particle in a non-spherical potential, i.e. Nilsson model states. Calculations of level spectra of odd-proton nuclei (Sholz and Malik, 1968), and an odd-neutron nucleus (Sanderson, 1973), close in mass to ^{71}Ge, have met with some success, with the assumption that the odd particle moves in a potential with a prolate deformation, with corrections for rotational-particle (Coriolis) coupling, and the effect of a pairing interaction between the core nucleons.

If the ^{70}Ge core is not permanently deformed, an alternative description of the states of ^{71}Ge can be formulated in terms of single-particle neutron states, generated by a

spherical potential, loosely coupled to the excitations of the ^{70}Ge core (Forssten et al., 1974). Some evidence for the spherical nature of the even-mass germanium isotopes can be seen in their level spectra. The level spectra of the heavier isotopes, ^{74}Ge and ^{76}Ge, have structures similar to those of a collective oscillator, i.e. a 0^+ ground state, a 2^+ first excited state, and a 0^+, 2^+, 4^+ triplet of states at about twice the excitation energy of the first 2^+ state. The level spectrum of ^{70}Ge departs considerably from the ideal model, though measurements of the quadruple moment of the first 2^+ state (Simpson et al., 1969), and the ratios of gamma-ray transition strengths (Simpson et al., 1971), are in good agreement with predictions of the vibrational model.

To make a meaningful comparison of the success of the different model calculations on ^{71}Ge, detailed information on the low lying level structure of this nucleus is required. A recent compilation by Alvar (1973) lists the experimental data available on ^{71}Ge at that time.

Some levels have been investigated by particle transfer reactions e.g. ^{70}Ge(d,p) ^{71}Ge (Goldman, 1968), and ^{72}Ge(p,d)^{71}Ge (Fournier et al., 1973) ; and level energies have been proposed, and values of the angular momentum of the transferred neutron have been deduced. More levels have been observed in the ^{71}Ga(p,n) ^{71}Ge and ^{71}Ga(p,n γ)^{71}Ge reactions (Malan et al., 1970), and a detailed gamma-decay scheme has been deduced, on the basis of neutron time-of-flight spectra, gamma-ray spectra

in coincidence with neutrons, gamma-ray threshold determinations and excitation functions, and gamma-gamma coincidence measurements. Some spin values were proposed, with qualitative arguments based on the relative strengths of population of the levels in ^{71}Ge in the (p,n) reaction.

The decay scheme of ^{71}Ge has been extended, and verified, by the study of gamma rays resulting from thermal neutron capture on ^{70}Ge (Weishaupt and Rabenstein, 1972), and the β decay of ^{71}As (Murray et al,1971., and Van Hise and Rainis, 1972).

From these studies, the placement of levels in ^{71}Ge and the gamma decay scheme were well known, but the spins and parities of many levels were unknown, or in doubt. The spin and parity assignments of the lowest three levels of ^{71}Ge were well established as $\frac{1}{2}^-$, $5/2^-$ and $9/2^+$, but spin assignments of higher levels were not firmly based, and some inconsistencies existed between the (d,p) and (p,d) data and the other studies.

While the work described in this thesis was underway, a description of further studies on the ^{71}Ga(p, n γ) ^{71}Ge reaction was published (Malan et al., 1974), with spin and parity assignments to most of the levels below 1.4 MeV excitation in ^{71}Ge. These assignments were made by measuring the relative populations of the states in ^{71}Ge fed by the (p,n) reaction, and the gamma-ray angular distributions of the decay of these states. Considerable reliance was placed

on the Statistical Compound Nucleus Reaction Model (Vogt, 1968) in calculating expected population strengths of the levels, and the distribution of population over the angular-momentum magnetic substates, as a function of excitation energy, spin and parity. The ^{71}Ga $(p,n\gamma)^{71}$Ge reaction is not well suited to determining spins of low spin states and gamma ray multipole mixing ratios from angular distribution measurements, because the spin of the ground state of ^{71}Ga is 3/2. Thus the states fed in ^{71}Ge will have an almost constant distribution of population, as a function of the angular-momentum magnetic substate quantum number m, up to, and including, the m = 5/2 substate; so the gamma-ray angular distributions from the decay of levels of spin 5/2 or less are expected to be all close to isotropic.

The ^{68}Zn$(\alpha,n\gamma)^{71}$Ge reaction provides a method of determining spins and mixing ratios with less reliance placed on the model of the reaction populating the states in ^{71}Ge. Both particles in the incident channel (the ^{68}Zn and alpha particle) have zero angular momentum, so if the outgoing neutron has low energy, the levels fed in ^{71}Ge will be highly aligned (as will be discussed in Chapter 2). The gamma-ray angular distributions will contain, potentially, more information than those seen in the ^{71}Ga$(p,n\gamma)^{71}$Ge reaction; e.g. it will be possible to determine multipole mixing ratios of gamma-ray transitions from low spin levels.

The ^{68}Zn $(\alpha,n\gamma)^{71}$Ge reaction has been studied previously at an alpha bombarding energy of 14 MeV (i.e. 7.4 MeV above threshold), with the aim of identifying some high spin states at relatively high excitation, which were expected to be of a simple structure (Forssten et al., 1974), but little information was provided on the lower-lying levels.

It was decided to investigate the lower-lying levels of ^{71}Ge by measuring gamma-ray angular distributions, and gamma-gamma correlations to provide an independent determination of the angular momenta of the levels of ^{71}Ge and multipole mixing ratios of gamma decays. A comparison of the experimentally deduced level structure of ^{71}Ge is made with the predictions of a model based on coupling neutron single particle states to the vibrations of a ^{70}Ge core.

CHAPTER 2

GAMMA-RAY DECAY

2.1 Introduction

The observation of gamma rays produced by the decay of nuclear levels which have been populated by a nuclear reaction provides a very powerful tool for studying nuclear levels. The spatial radiation pattern, or angular distribution, of a gamma ray can frequently be used to determine, or restrict the possible values of one of the spins of the levels involved in the transition, if the other spin is known. The ratio of the reduced transition probabilities of the different gamma-ray multipolarities (the mixing ratio) can often be determined; and compared with the predictions of nuclear models. In many cases the observation of the angular distribution alone is not sufficient to uniquely determine the unknown spin and mixing ratio, but other techniques can be used to remove some of these ambiguities. For example, the observation of the relative angular distribution, or correlation, of two gamma rays emitted in a cascade provides further information on the spins and mixing ratios involved in the decay.

The theory of gamma-ray decay has been well developed and described elsewhere (e.g. Rose and Brink, 1967, and Ferguson, 1965), so only a summary of the relevant results is

presented here.

2.2 Angular Distributions

Consider a reaction induced by an unpolarized beam of particles of type 'a' incident on a nucleus of type 'A', in which a particle 'b' is emitted, leaving the final nucleus 'B' in an excited state i.e. $A(a,b)B^*$, in which all the states a, A, b and B^* have sharp angular momentum. The excited state, B^*, then decays by gamma-ray emission. If the outgoing particle 'b' is undetected, and the nucleus B^* decays sufficiently rapidly that it is relatively unaffected by the presence of any electromagnetic fields in the target material, then there will be axial symmetry around the direction defined by the incoming beam. The ensemble of nuclei of type B^* can be parameterized by the proportion of these nuclei which exist in each substate of angular-momentum projection quantum number 'm' along the z axis defined by the beam direction. These so-called 'population parameters', $w(m)$, are determined by the mechanism of the reaction producing the nuclei B^*. If parity is conserved in the reaction $A(a,b)B^*$, then the population parameters satisfy the requirement that $w(m) = w(-m)$, and the ensemble is said to be aligned.

The angular distribution of the gamma rays from the decay of the aligned ensemble of states, B^*, to some lower state, measured with a detector insensitive to the polarization of the gamma rays can be written:

$$W(\theta) = \Sigma_k A_k P_k(\cos \theta) \qquad (2.1)$$

where the P_k functions are Legendre polynomials of order k, and θ is the angle between the direction of observation of the gamma ray and the incoming beam direction. The index k takes on only even values and is restricted by the conditions.

$$k \leq 2J_1$$
$$k \leq 2L' \qquad (2.2)$$

where J_1 is the angular-momentum quantum number of the initial decaying state, and L' is the highest multipole in the multipole expansion of the electromagnetic field, involved in the decay.

Assuming that only two multipolarities contribute to the decay, the expansion coefficients, A_k, are related to the population parameters of the initial state and the spins of the levels involved in the decay by:

$$A_k = B_k(J_1) \left\{ \frac{R_k(L\ L\ J_1 J_2) + 2\delta\ R_k(L\ L'\ J_1 J_2) + \delta^2 R_k(L'L'\ J_1 J_2)}{1 + \delta^2} \right\}$$

with $B_k(J_1) = \sum_m w(m)\ (-)^{J_1 - m} \sqrt{(2J_1 + 1)}\ (J_1\ m\ J_1 - m | ko)$ (2.3)

and $R_k(L\ L'\ J_1 J_2) = (-)^{1 + J_1 - J_2 - L + L'} \dfrac{-k}{\sqrt{(2J_1+1)(2L+1)(2L'+1)}}$

$\qquad\qquad \times (L\ 1\ L'\ -1 | ko)\ W(J_1 J_1 L\ L'\ ;\ kJ_2)$

where J_1 and J_2 are the angular-momentum quantum numbers of
the initial and final nuclear levels, and L and L' are the
two multipolarities of the radiation involved in the decay.
The mixing ratio is given by:

$$\delta = \frac{\langle J_1||T_{L'}||J_2\rangle}{\langle J_1||T_L||J_2\rangle} \times \left(\frac{2L+1}{2L'+1}\right)^{\frac{1}{2}} \qquad (2.4)$$

where the matrix elements $\langle J_1||T_L||J_2\rangle$ are the reduced
transition probabilities for the two multipolarities L and
L' = L + 1.

The functions $(Jm\ J-m|ko)$ and $W(J_1J_1L\ L';kJ_2)$ are
Clebsch-Gordon and Racah coefficients.

The order of the multipolarity of the radiation gives
the angular momentum carried off by the electromagnetic field,
so;

$$|J_1 - J_2| \leqslant L,\ L' \qquad (2.5)$$

The radiation can be classified according to whether
it is induced by the distribution of charges (an electric
transition) or currents (a magnetic transition) within the
nucleus. The transition matrix elements are zero unless the
products of the parities of the initial and final nuclear
levels are $(-1)^L$ for electric radiation, or $(-1)^{L+1}$ for
magnetic radiation.

Normally it is sufficient to consider only L = 1 and L' = 2 multipole radiations, so the index k in equation 2.1 is restricted to the values 0, 2 and 4. In the experiments described the absolute intensities of the gamma rays were not measured, so experimentally only the quantities $a_2 = A_2/A_o$ and $a_4 = A_4/A_o$ were determined for each distribution.

In measuring the distribution experimentally, the gamma-ray detectors have a finite entrance aperture, so they measure the angular distribution averaged over a small range. In the case of a detector which has cylindrical symmetry the averaging effect can be allowed for by calculating attenuation coefficients, Q_k, for the detector, at the target-detector distance chosen. The observed distribution is then given by:

$$W(\theta) = \Sigma_k A_k Q_k P_k(\cos\theta) \qquad (2.6)$$

The Q_k coefficients have been tabulated for various detector sizes and source-detector distances (Camp, 1968).

2.3 Angular Correlations

The observation of one angular distribution of a gamma-ray decay will only provide sufficient information to unambiguously determine the unknown parameter of the decay in certain favourable circumstances. Generally more than one choice of the unknown spin and mixing ratio will reproduce the experimentally determined a_2 and a_4 coefficients of the

distribution.

As pointed out previously in this chapter, such ambiguities can sometimes be resolved by measuring the relative angular correlation at two gamma rays emitted in a cascade. The angular correlation is a function of three angles, usually taken as the angles between the incoming beam direction and the directions of the outgoing gamma rays (θ_1 and θ_2), and ϕ, the angle between the two planes defined by each of the outgoing gamma rays and the beam direction.

The expression for the angular correlation from an initially aligned state is then given by (Ferguson, 1965):

$$W(\theta_1,\theta_2,\phi) = \sum_{k_1k_2k_3} a_{k_1k_2k_3} P_{k_1k_2k_3}(\theta_1,\theta_2;\phi) \qquad (2.7)$$

where the indices k_1, k_2, k_3 are restricted to the values 0, 2 and 4, if the maximum multipolarity of the emitted radiations is 2. The coefficients $a_{k_1k_2k_3}$ are determined by the spins and mixing ratios involved, and the population parameters of the initial state. The $P_{k_1k_2k_3}$ functions are sums of products of spherical harmonic functions of the angles θ_1, θ_2 and ϕ. These functions simplify considerably if the angles θ_1, θ_2 or ϕ are suitably chosen. Ferguson lists seven such detector configurations, or 'geometries', in which two of the angles are fixed at 0°, 90° or 180° to the beam direction, while the third is varied. The $P_{k_1k_2k_3}$ functions can then be written:

$$P_{k_1 k_2 k_3} = \sum_k \alpha^k_{k_1 k_2 k_3} P_k'(\cos \theta) \qquad (2.8)$$

where θ is the variable angle, and the $\alpha^k_{k_1 k_2 k_3}$ coefficients are tabulated by Ferguson for the different geometries.

The expression for the correlation then reduces to a sum over even order Legendre polynomials, up to order 4.

2.4 Alignment and the Compound Nucleus Statistical Model

The previous discussion of gamma-ray angular distributions and correlations presumes that the initial state, which gamma decays, is aligned, i.e. $w(m) = w(-m)$, but in general $w(m) \neq w(m')$. It is advantageous to the analysis of the experimental data that the coefficients a_2 and a_4, in the expressions for the angular distributions, be as large as possible, so they can be determined most accurately. This occurs when the alignment of the initial state is highest, i.e. when there is a high probability that the initial state is in a substate of low 'm' value.

The (α,n) reaction on a spin-zero target can produce highly-aligned states, particularly when the alpha-particle energy is not far above the threshold of the reaction. Since the direction of the incoming alpha particle is along the axis of quantisation, the projection of its orbital angular momentum on the z axis is zero. If the incoming alpha-particle energy is such that the outgoing neutron has low energy, then

it will be emitted predominantly in the $\ell = 0$ partial wave, and hence will carry off only half a unit of angular momentum. Thus the residual nucleus will have a high probability of being in the $m = +\frac{1}{2}$ or $m = -\frac{1}{2}$ substate, i.e. the state will be aligned.

Best alignment will be obtained when the emitted neutrons have very low energy, but generally the yield from the reaction is too low to enable gamma-ray distributions to be measured accurately unless the emitted neutrons have energies of over 500 keV. In such cases a significant proportion of the outgoing neutrons will be emitted with non-zero orbital angular momentum, and so substates having m values greater than $\frac{1}{2}$ can be populated. The residual nuclei will still be aligned, and hence their gamma decays will in general show non-isotropic angular distributions, but the analysis of the experimental results will have to allow for the effect of the population of the higher substates, and a method of calculating the distribution of population over the substates is required.

It has been demonstrated that the Compound Nucleus Statistical Reaction Model can accurately predict the population parameters and hence the gamma-ray angular distributions resulting from (α,n) reactions, in the energy range and mass region used in the present study (Birstein et al, 1968). The physical basis and development of the Compound Nucleus Statistical Model has been well described elsewhere (Sheldon and Van Patter, 1966 and Vogt, 1968), and only an outline is

presented here.

From general reaction theory, the cross section of
a nuclear reaction can be expressed in terms of the elements
of the reaction matrix $U_{cc'}$, which relates the amplitudes,
$B_{c'}$, of outgoing partial waves produced in a reaction to the
amplitudes, $A_{c'}$, of the incoming partial waves of the incident
particle, thus

$$B_c = \Sigma_{c'} U_{cc'} A_{c'} \qquad\qquad (2.9)$$

The labels c and c' include all the quantum numbers
necessary to specify a partial wave in a reaction channel,
i.e. particle type, orbital angular momenta, total angular
momenta etc. The cross section leading to a particular state
of given angular momentum and angular momentum projection
quantum number m, in which the outgoing particle is unobserved,
is given by a sum over $|U_{cc'}|^2$, weighted by angular-momentum
coupling coefficients. The summation is taken over all
possible angular-momentum quantum numbers describing the
process, consistent with conservation of total angular momentum
and parity. The compound nucleus model of reactions presumes
that the reaction proceeds through resonances in the compound
state of the target plus incident particle, and the elements
of the matrix $U_{cc'}$ are given by a summation of the contribution
from the resonances;

$$U_{cc'} = -\sum_\lambda \frac{\Gamma_{\lambda c}^{\frac{1}{2}} \Gamma_{\lambda c'}^{\frac{1}{2}}}{E_\lambda - E - \frac{i\Gamma_\lambda}{2}} \qquad (2.10)$$

where E_λ is the energy of a resonance in the compound system, having widths $\Gamma_{\lambda c}$ and $\Gamma_{\lambda c'}$ for decay into the c and c' channels, and total width Γ_λ.

At low excitation energies the resonances are separated from each other by energies greater than the widths (Γ) of the resonances, so the cross section, as a function of energy, shows the effect of each resonance individually. At higher excitation energies the widths increase and the resonance spacings decrease until the individual resonances strongly overlap and interfere. The reaction cross sections at these higher energies fluctuate (Ericson, 1963) with the energy spacing of the fluctuations, or coherence width, being of the order of the average level width Γ. In this region of fluctuating cross sections it is not useful to describe the cross sections in terms of the parameters of the individual resonances, only statistical quantities, such as averaged cross sections are meaningful.

If it is assumed that the widths and energies of the compound resonances are both randomly distributed, and un-correlated, then the value of $|U_{cc'}|^2$, averaged over energy, can be expressed as:

$$\langle \, |U_{cc'}|^2 \, \rangle = 2\frac{\pi}{D} \cdot \frac{\langle \Gamma_{\lambda c} \rangle \langle \Gamma_{\lambda c'} \rangle}{\langle \Gamma_\lambda \rangle} \tag{2.11}$$

where $\langle \ \rangle$ denotes 'average value over energy', and D is the average spacing of the resonances. This can be expressed as

$$\langle \, |U_{cc'}|^2 \, \rangle = \frac{T_c \, T_{c'}}{\Sigma_{c''} T_{c''}} \tag{2.12}$$

where
$$T_c \equiv 2\pi \, \frac{\langle \Gamma_{\lambda c} \rangle}{D}$$

where T_c is the averaged probability for decay of the compound nucleus into channel c, and the summation $\Sigma_{c''} T_{c''}$ is taken over all decay channels permitted by conservation laws. These functions, T_c, are calculated in the statistical reaction model by taking them as being equal to transmission coefficients for partial waves incident on an optical model potential. The potentials are those which describe elastic scattering of the incident particle plus target, or outgoing particle plus residual nucleus, system. If these potentials have no spin-dependent term, i.e. the transmission coefficients depend only on the orbital angular momentum ℓ, then, according to Vogt(1968) the cross section of a reaction populating a state of spin J_f and spin-projection m, induced by a projectile of spin i on a target of spin I, is given by:

$$\sigma(J_f, m) = \frac{1}{4k_\alpha^2(2I+1)(2i+1)} \sum_{ss'm_s m_s'} \sum_{J\ell\ell'} (2\ell+1)(2\ell'+1)(\ell s m_\ell m_s | J m_s)^2$$

$$x \; (\ell's'm_\ell'm_s'|Jm_J)^2(\ell 0 00/00) \frac{T_\ell(\alpha) \, T_{\ell'}(\alpha')}{\sum_{\alpha''\ell''s''} T_{\ell''}(\alpha'')} \qquad (2.13)$$

where k_α is the wave number for the initial system, s, m_s, s' and m_s' are channel spins and channel-spin projections in the initial and final channels, ℓ and ℓ' are orbital angular momenta, and J is the total angular momentum of the system. The summation is taken over all the quantum numbers allowed by conservation of angular momentum, its projection, and parity. The term $\sum_{\alpha''\ell''s''} T_{\ell''}(\alpha'')$ is taken over all open exit channels.

Thus the statistical model allows relative populations of different m states in the final nucleus to be calculated.

The statistical model predicts energy-averaged cross sections, so its use should be restricted to describing reactions where experimentally an average is taken over some energy interval, ΔE, of bombarding energy, where ΔE is much larger than the average level spacing and width in the compound nucleus. This can be achieved in the (α,n) reaction by using a thick target in which the incident beam loses energy, so that effectively the incident beam has an energy spread. Because the energy-averaging interval, ΔE, in a real

experiment is finite, statistical fluctuations can appear in the measured cross sections, whose magnitude can be estimated. Under the assumptions of the statistical compound nucleus model the squares of the elements of the reaction matrix $|U_{cc'}|^2$ fluctuate as a function of energy with a χ^2 distribution with two degrees of freedom, i.e. the probability distribution of $|U_{cc'}|^2/<|U_{cc}|^2>$ is given by (Ericson and Mayer-Kuckuk, 1966)

$$P(x)\ dx\ =\ e^{-x}\ dx \tag{2.14}$$

with

$$x\ =\ |U_{cc'}|^2/<|U_{cc'}|^2>$$

Experimentally a sample average of $|U_{cc'}|^2$ is taken, denoted $<|U_{cc'}|^2>_s$, over an energy range ΔE, containing N independent samples of $|U_{cc'}|^2$, where

$$N\ =\ \Delta E/\pi\Gamma \tag{2.15}$$

where Γ is the average level width.

The probability distribution of $<|U_{cc'}|^2>_s/<|U_{cc'}|^2>$ then has a χ^2 distribution with 2N degrees of freedom. For large N this distribution approaches a normal distribution having a standard deviation of $1/\sqrt{N}$ i.e. the experimental values of $<|U_{cc'}|^2>_s/<|U_{cc'}|^2>$ show fluctuations of the order $1/\sqrt{N}$.

2.5 Methods of Analysis

A postulated set of spins and mixing ratios involved
in a gamma decay can be tested against experiment by comparing
the predicted angular distributions (and/or correlations)
against the experimentally determined distributions. As
described previously, the theoretical distributions depend on
the angular momenta of the nuclear levels involved, the mixing
ratios, and the population parameters of the initial state.
The usual technique of analysis involves choosing initial and
final spins and population parameters, and stepping the mixing
ratio, δ, from $-\infty$ to $+\infty$ (or arctan δ from -90° to $+90^{\circ}$).
The theoretical distribution at each value of δ is calculated,
normalised to give the same A_0 coefficient as the experimental
data, and compared with the experimental distribution. The
quality of the fit to the data is gauged by the parameter 'S',
where

$$S = \sum_i \left(\frac{W_i - Y_i}{\sigma_i}\right)^2 \qquad (2.16)$$

where W_i is the theoretically predicted value of the distrib-
ution at one angle, Y_i is the corresponding measured value,
and σ_i is the variance in Y_i.

A difficulty arises in the analysis because the
population parameters are not known exactly, only estimates
are available from the statistical reaction model. These
estimates could be in error because of statistical fluctuations
in the cross sections; or a poor choice of the optical model

parameters ; or cascade feeding of the level of interest by
gamma decays from higher-lying levels. A commonly used
technique in the analysis of such data allows the population
parameters to vary, within somewhat arbitrarily chosen limits,
at each chosen value of δ, to find the minimum value of S for
that δ. A more satisfactory technique has been described by
James et al. (1974). At each choice of δ the population
parameters, w(m), are allowed to vary to minimise S, defined
by:

$$S = \sum_i \left(\frac{Y_i - Y_i}{\sigma_i}\right)^2 + \sum_m \left(\frac{w(m) - e(m)}{\Delta(m)}\right)^2 \qquad (2.17)$$

subject to
$$\sum_{m=-J}^{+J} w(m) = 1$$

and
$$0 < w(m) < .5$$

and
$$w(m) = w(-m)$$

In equation 2.17 e(m) is the estimated value of the population
of the m substate and $\Delta(m)$ is an estimate of the allowed
variation in the population parameter. (The summation over m
in equation 2.17 in the expression for S omits the lowest
value of m.) Thus the population parameters are permitted to
vary, but the second term in the expression for S prohibits
fits to the data from being obtained which require population
parameters far from those predicted by the statistical model.

If the errors in the experimentally determined data points are normally distributed, and if true values of the spins and mixing ratio are chosen, then S/ν has a χ^2 distribution with ν degrees of freedom; where ν is the difference between the number of data points and the number of independent free parameters in the theory. A choice of spins is judged as providing a possible description of the data if, for some value of the mixing ratio, the statistic S falls below the .1% confidence limit for χ^2, i.e. the chance of rejecting the correct choice of spins and mixing ratio is 1 in 1000.

If the curve of $\chi^2 = S/\nu$ against arctan δ, for some chosen initial and final nuclear spins, falls below the 0.1% confidence limit, then the best estimate of arctan δ for the transition is at the minimum value of χ^2 (χ^2_{min}). The standard error on arctan δ is determined by the intersection points of the χ^2 curve with the line ($\chi^2_{min} + 1$).

CHAPTER 3

EXPERIMENTAL METHODS

3.1 Introduction

The experiments fall into two types (i) singles measurements and (ii) coincidence measurements.

In the singles measurements all the gamma rays arising from the bombardment of a ^{68}Zn target with alpha particles were detected with lithium-drifted germanium (Ge(Li)) detectors, in order to measure gamma-ray energies, branching ratios, and angular distributions.

In the coincidence measurements only those gamma rays were counted which were detected in one detector accompanied by another gamma ray in a different detector. This permitted the decay scheme of ^{71}Ge to be further elucidated, and gamma-gamma correlations to be measured.

3.2 Singles Measurements

3.2.1 Preliminaries

In these measurements a beam of alpha particles produced by the McMaster University FN Tandem Accelerator was collimated by tantalum apertures , to give a beam spot of less than 1.5mm diameter, and directed onto a target mounted in the centre of a stainless steel evacuated chamber. The targets consisted of

zinc metal, enriched to greater than 99% in the ^{68}Zn isotope, on a gold backing, of thickness $.5 \times 10^{-3}$ inches. The gamma rays produced by the interaction of the beam with the target were detected with Ge(Li) detectors, the signals from which were amplified by low-noise shaping amplifiers, and converted to digital form by analogue-to-digital converters (ADC's) with 4096 channels. The ADC words were read by a PDP-9 computer, which accumulated spectra, displayed these spectra on a cathode ray display, and wrote the spectra onto magnetic tape for further analysis at the end of a run. The computer programs for data acquisition are described in some detail in appendix A.

The energies of the gamma rays from the reaction were accurately determined by simultaneously collecting data from the ^{68}Zn$(\alpha, n\gamma)^{71}$Ge reaction, and from gamma-ray sources of ^{56}Co, ^{54}Mn, ^{137}Cs, ^{228}Th and ^{182}Ta. The variation of efficiency of the detectors with gamma-ray energy was measured with ^{56}Co and ^{182}Ta sources.

A preliminary measurement was made with a relatively thin target, of about 100 μgm/cm^2 thickness, corresponding to an energy loss in the incident beam, when traversing this thickness, of about 30keV at 8MeV bombarding energy. The beam energy was stepped from 8 MeV to 10MeV in 100keV steps to verify that the reaction cross section varied smoothly with energy; a pre-requisite for the application of the statistical model.

3.2.2 Angular Distributions

The Q value of the $^{68}Zn(\alpha,n)^{71}Ge$ reaction is
– 5.738 MeV. To provide an adequate counting rate to the
levels of interest, alpha – bombarding energies of 8.0 and
8.5 MeV were used. The target thickness was 1.4 mgm/cm^2,
corresponding to an energy loss of 400 keV in the incident
beam, so that a large number of coherence widths in the com-
pound nucleus were averaged over. Beam currents were
held to 300 nA to minimise deterioration of the target material.
The gamma-ray angular distributions were measured with a
Ge(Li) detector, of active volume 14cc, having a resolution
of 2.5 keV at 1.33 MeV, set at a distance of 12cm from the
target. Spectra were recorded at angles of 0°, 144°, 125°,
110° and 90° to the incident beam direction. A monitor
detector of 50cc active volume was kept at a fixed angle to
the beam, so that data taken by the 14cc moveable detector
could be normalised to the same product of (number of incident
particles) x (number of target nuclei). Eventually it was
shown, in the gamma-gamma correlation work, that the spin of
the 808 level in ^{71}Ge is $\frac{1}{2}$, so the gamma decays from this
level must be isotropic. Thus the final normalisations were
taken from the decay of the 808 level to the ground state
and the 500 keV state. This method of internal normalisation
avoids certain sources of systematic errors, such as dead-
time correction in the ADC's.

The peak areas in the spectra were measured either using the program JAGSPOT, on the CDC 6400 computer, which fits an analytic form to the peaks plus background; or with an interactive program, using a display and light-pen, on a PDP-15 computer, which fitted an analytic form to the background region around a peak, and subtracted background from under the peak.

3.3 Coincidence Measurements

A beam of 10MeV alpha particles initiated a reaction on a ^{68}Zn target of 2.5 mgm/cm^2 thickness. The gamma rays from the reaction were viewed with two detectors. One of these, a 65cc Ge(Li) was kept fixed at 90° to the beam direction; the other, a 50cc Ge(Li) was positioned at angles 0°, 147°, 135°, 120° and 90° to the beam direction. This arrangement allowed coincidence data from the two geometries referred to as A1 and A2, by Ferguson (1965) to be collected. A cascade of two gamma rays in which the first gamma ray is detected in the moving detector, and the second in the 90° detector, is in the A1 geometry. The A2 geometry corresponds to the case when the first gamma ray, enters the fixed 90° detector.

The electronics configuration is shown in Figure 3.1. If a coincidence event (within the resolving time set by the single channel analyser SCA(1) on the time-to-amplitude converter output) was detected then the energy signals from the detectors, and the TAC output, were digitised by ADC's

and read by a PDP-9 computer. The computer stored all the
digitised information in its memory, until a number of events
had been collected, then dumped all the information onto
magnetic tape. The program used for accepting and storing
data in this 'event-by-event' mode is described in Appendix A.

Data were collected at each angle setting of the 50cc
detector until one 2400ft reel of magnetic tape was filled
with data, corresponding to about one million coincidence
events. The measurement at each angle was repeated at least
once, and in some cases, twice.

A program (described in Appendix B) was written for
a PDP-15 computer to play back the data on the magnetic tape.
Digital windows were set on the total accumulated spectra
(the projected spectra) of the 50cc detector, on each peak
of interest, and on background regions adjacent to each peak.
Windows were also set on the TAC spectra on regions corres-
ponding to 'true plus chance' events and 'chance' coincidence
events. The tapes were then scanned to produce spectra from
the 65cc detector for each peak window set on the 50cc
detector, corrected for both background and random coincidence
events.

Angular correlations were constructed by measuring the
areas of the more prominent peaks in the spectra. Normali-
sations between the runs at different angles were taken from
spectra which had been collected in singles mode, by the
fixed detector, during the coincidence runs.

FIGURE 3.1

A block diagram of the electronics used in the gamma-gamma coincidence experiment, constructed from commercially-available NIM modules.

EZS = Extrapolated Zero Strobe

AMP = Amplifier

LGS = Linear Gate and Stretcher (to delay and shape pulses)

TAC = Time-to-Amplitude Converter

DLY = Delay

SCA = Single Channel Analyser

SCLR = Scaler

LSD = Logic Shapes and Delay

ADC = Analogue-to-Digital Converter

ADC I

ADC 3

Gate on ADC's 1,2 & 3

ADC 2

Singles Monitor ADC

Gate on Monitor ADC

LGS

DLY

LSD

LGS

DLY

LSD

AMP

SCA(1)

AMP

SCA(2)

TAG

DLY

START

STOP

EZS

EZS

SCLR

γ

γ

65 cc Ge(Li)

^{68}Zn target

50 cc Ge(Li)

α beam
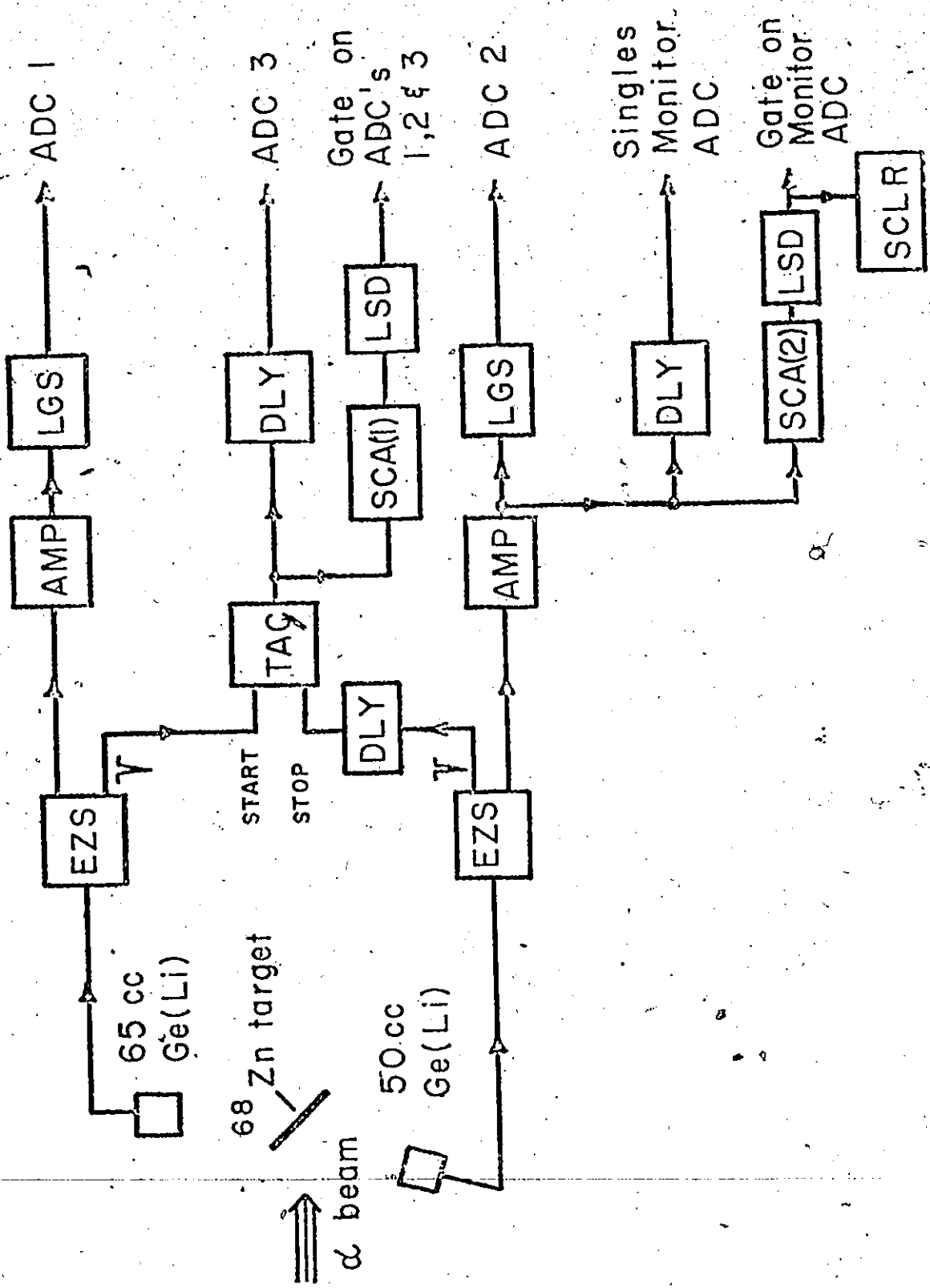
CHAPTER 4

EXPERIMENTAL RESULTS AND ANALYSIS

4.1 Preliminaries

Figure 4.1 shows the low-lying level scheme of ^{71}Ge,
with the gamma rays observed in this work, either seen in the
singles studies, the coincidence studies, or both.   The
energies of the gamma rays determined in this work agree with
those determined by Malan et al (1974), within experimental
errors, so the energies quoted by them are used.   The angular-
momentum quantum numbers and parities of the lowest three
states of ^{71}Ge have been shown to be $1/2^- 5/2^-$ and $9/2^+$; the
spins determined by the present work are indicated in figure
4.1.

4.2 Singles Measurements

A spectrum obtained from the ^{68}Zn$(\alpha, n\gamma)^{71}$Ge reaction
at a bombarding energy of 8.0 MeV is shown in figure 4.2.
The lines recognised as gamma rays from ^{71}Ge are labelled
with the energies of the initial and final nuclear levels in
^{71}Ge.   The lines labelled ^{197}Au, ^{181}Ta and ^{68}Zn arise from
gamma de-excitation of nuclei in the target backing, the
apertures and the target which have been excited by inelastic
scattering of alpha particles.   The lines labelled ^{19}F, ^{26}Aℓ
and ^{23}Na are derived from the ^{19}F$(\alpha, \alpha')^{19}$F*, ^{23}Na$(\alpha, n)^{26}$Aℓ

and $^{23}Na(\alpha, \alpha')$ $^{23}Na^*$ reactions, due to impurities in the target material, or backing.

Angular distributions were measured of the gamma rays which appeared with sufficient intensity, which were fitted to the function:

$$W(\theta) = \sum_{k} A_k Q_k P_k(\cos \theta)$$

with $Q_2 = .980$ and $Q_4 = .930$. The A_o coefficients were corrected for detector efficiency effects, and branching ratios of the decays of the levels were calculated. When the gamma ray was not sufficiently intense to allow the angular distribution to be measured, the peak area of the gamma ray determined in a measurement at an angle of 125° was used, since the P_2 Legendre polynomial is zero at this angle. The branching ratios are summarised in table 4.1. The errors include the statistical errors on the A_o coefficients and possible errors in the calibration of the efficiency of the detector. In general the measurements agree with those of Malan et al (1974), within the errors. The a_2 and a_4 coefficients of the fitted distributions are presented in table 4.2. The coefficients given for the 808, 308, and 633 keV gamma rays were obtained by normalising between different runs using the monitor detector. The other distributions were normalised assuming that the 308 and 808 lines were isotropic.

4.3   Coincidence Measurements

A spectrum of the counts in the 65 cc detector in coincidence with the 500 keV line in the 50 cc detector, corrected for background and chance contributions, is shown in figure 4.3.   Transitions which cascade through the 500 keV level from the 808, 747, 1026 and 1289 keV levels can clearly be seen.   Angular correlations of the stronger lines in the coincidence spectra were fitted to an expansion of even-order Legendre polynomials, the coefficients of which are presented in table 4.3, for the two geometries A1 and A2.

4.4   Spin assignments from Distributions and Correlations

4.4.1   Choice of Population Parameters

The population parameters of the initial states in the gamma-ray decays were calculated using the Statistical Compound Nucleus computer code AK (Green, 1971), which was derived from the code MANDY by Sheldon and Strang (1969). The transmission coefficients used as input to this program were calculated by the computer code ABACUS.   The optical model parameters for the alpha plus ^{68}Zn, and neutron plus ^{71}Ge systems were taken from compilations, derived from analysis of elastic scattering experiments (Perey and Perey, 1974 and Bjorkland and Fernbach, 1958).   Typically the population parameters of states in ^{71}Ge of spins greater than 3/2 were predicted to be $w(\pm \frac{1}{2}) = .32$, $w(\pm 3/2) = .14$ and $w(\pm 5/2) = .04$. The theoretical angular distributions and correlations, as

functions of spins and mixing ratios, were calculated using
the program LISA, written by P.W. Green on a PDP-15 computer,
which minimised the quantity S defined in equation 2.17.
A choice of the permitted variations, $\Delta(m)$, in the calculated
population parameters had to be made. Possible sources of
the variations are discussed below.

The effect of statistical fluctuations on the
calculated population parameters is expected to be negligible,
since an excitation function of the $^{68}Zn(\alpha,n\gamma)$ Ge reaction
using a thin target was smooth, within experimental errors.
Furthermore, a plot of Γ (the average level width) against
$(A/U)^{\frac{1}{2}}$ given by Ericson and Mayer-Kuckuk (1966) where A is
the mass number of the compound nucleus, and U is the
excitation energy, gives Γ as being about .2 keV in the case
of interest, which is to be compared with the energy loss
of the beam in the target of about 400 keV.

Cascade feeding of levels by gamma decay from higher-
lying levels alters the population parameters from those
obtained by direct neutron feeding only. Calculations on
typical cases indicate that this effect changes the relative
population parameters by at most 5% of the population of
the m = 3/2 substate.

Variations in the optical model parameters produce
little change in the population parameters. The parameter
describing the allowed variation of the m = 3/2 substate
was taken as 10% of the predicted population, i.e. $\Delta(3/2) = .014$,

and $\Delta(5/2)$ was taken as .01. A justification for taking values no larger than these was provided by the measured distribution of the decay of the 747 keV level of ^{71}Ge. Even allowing large variations in the population parameters the level spin could be determined as being 5/2. The decay of this level to the spin $\frac{1}{2}$ ground state is expected to proceed only by quadrupole radiation, i.e. the mixing ratio is fixed. Thus there are only two variable quantities describing the transition, the population parameters of the m = 3/2 and m = 5/2 substates. There are two experimentally determined quantities from the angular distribution of the transition, the a_2 and a_4 coefficients. Thus, knowing a_2 and a_4, the two unknown population parameters can be calculated. When the population parameters were calculated in this manner they were found to agree with those predicted by the statistical model, within the limits described above.

The spin assignments to the individual levels in ^{71}Ge are now discussed. Information from the correlation data is only presented when it provides additional information to that provided by the angular distributions.

4.4.2 500 keV Level

The angular distribution of the gamma decay of this level to the ground state (figure 4.4) unambiguously assigns a spin of 3/2 to this level, in agreement with the ^{71}Ga(p,nγ)^{71}Ge work of Malan et al. (1974), who based the assignment on the

angular distribution of the decay to the 500 keV level from the 747 keV level of spin 5/2. Angular distributions from the ^{70}Ge(dp)^{71}Ge (Goldman, 1968) and ^{72}Ge(p,d)^{71}Ge (Fournier et al, 1973) reactions agree that the transferred neutron has $\ell = 1$, indicating that the level has negative parity.

4.4.3 525 keV Level.

Gamma decays from this level to the 5/2$^-$ level at 175 keV, and the 9/2$^+$ level at 198 keV are seen. A decay from the spin 3/2 level at 831 keV to the 525 keV level is also observed, so, if at most quadrupole (L = 2) radiation is expected, the possible spin value of the 525 keV level is limited to 5/2 or 7/2. Angular distributions of the decays from the 525 keV level permit both spin possibilities at the .1% confidence level (figure 4.5), though the 5/2 value is clearly preferred in the 525 to 175 keV decay. The decay from the 831 keV level (figure 4.12) fixes the 525 keV level spin as 5/2.

Malan et al., assign a spin of 5/2 to this level on the basis of the angular distributions and the strength of the population of the level in the ^{71}Ga(p,nγ)^{71}Ge reaction. The (d,p) work of Goldman shows an $\ell = 2$ stripping pattern to this level, indicating positive parity.

4.4.4 590 keV Level

One decay is seen from this level, to the 9/2$^+$ 198 keV level, and a decay from the spin 3/2 831 keV level is observed. The angular distributions of the two decays (figures 4.6 and 4.12) allow a spin of 5/2 or 7/2 for the 590 keV level.

Malan et al. assign a spin of 7/2 to the level, with a preference for positive parity.

4.4.5 708 keV Level

The decay of this level to the ground state has an isotropic angular distribution, within experimental errors, allowing a spin of ½ or 3/2 (figure 4.6). Malan et al. assign 3/2$^-$, on the basis of intensity measurements. The (d, p) stripping reaction to this level shows an $\ell = 1$ angular distribution, indicating negative parity.

4.4.6 747 keV Level

Three gamma decays are seen from this level, to the ground state, the 175 keV state, and the 500 keV state (figures 4.7 and 4.8). The angular distribution of the latter decay unambiguously assigns a spin of 5/2 to the 747 keV state, in agreement with Malan et al., who give a preference for negative parity. According to the compilation by Alvar (1973), the negative parity assignment is confirmed by the observation of an $\ell = 3$ pattern in the (d,p) stripping reaction.

4.4.7   808 keV Level

Figures 4.9 and 4.10 show angular distributions of the three gamma transitions observed from this level, to the ground state, the 175 keV state and the 500 keV state, normalised to the monitor counter. The best fits to the data are obtained with an initial-state spin of ½ or 3/2. The gamma-gamma cascade from the 808 keV level through the 500 keV level to ground was strong enough to allow angular correlations to be measured. Figure 4.10 shows how the spin of the 808 keV level can be determined as ½ by considering the angular distributions and correlations simultaneously. The correlations as shown in figure 4.10 were calculated with arctan δ of the 500 keV to ground transition set at -7°; the alternative selection of 67° provides an equally good determination of the spin of the 808 keV level.

Malan et al. assign ½⁻ to this level, from intensity considerations. An assignment of $\ell = 2$ in the (d,p) work of Goldman (1968), on the basis of a very weakly populated angular distribution has not been substantiated by later work (Alvar, 1973).

4.4.8   831 keV Level

The decay to the ground state from this level unambiguously assigns a spin of 3/2, in agreement with Malan et al., who also suggest positive parity.

4.4.9 1026 keV Level

The angular distribution of the decay to the 500 keV level (figure 4.13) allows only a spin of 5/2 for the 1026 keV level. Malan et al. assign 5/2⁻ to this level.

4.4.10 1038 keV Level

Two gamma transitions from this level were identified, but neither angular distribution could be measured sufficiently accurately to provide useful information.

4.4.11 1095.5 keV Level

The decay of this level to the ground state was insufficiently intense to allow an angular distribution to be measured. The level is expected to have low spin because it is populated in the β-decay of ^{71}As (Murray et al., 1971). Malan et al assign a spin of 3/2⁻.

4.4.12 1096.0 keV Level

The large a_2 and a_4 coefficients of the angular distribution of the decay to the 5/2⁻ 175 keV level indicate that the 1096.0keV level has a high spin, and so cannot be identified as the low-spin 1095.5 keV level.

According to Murray et al. (1971) the 1095.5 keV level also has a gamma-decay branch to the 175 keV level. The gamma-detector resolution used in the ^{68}Zn(α,nγ)^{71}Ge experiment was insufficient to distinguish between the decays of the 1095.5 keV

and 1096 .0keV levels to the 175 keV level, so the angular
distribution of the sum of the two peaks was measured.
Using the measured peak area of the 1095.5 keV to ground
transition, and the branching ratio of the decay of the
low-spin 1095.5 keV level to the ground and 175 keV states
as determined in the ^{71}As β-decay studies (Murray et al., 1971),
it was calculated that the low spin decay contributed about
8% of the measured peak areas. The anisotropy (or the a_2
coefficient) of the distribution of the decay of the low
spin level is unknown, but limits can be set on it, assuming
that the initial state spin is 3/2. For any possible anisotropy
of the 1095.5 keV decay, the corrected angular distribution
of the 1096.0keV to 175 keV decay was found to be only
consistent with an initial-state spin of 7/2. Figure 4.14 shows
the angular distribution corrected for an isotropic contrib-
ution from the low-spin decay. Malan et al. also assign a
spin of 7/2.
 The strength of the transition to the 3/2$^-$ 500 keV
level suggests negative parity for the 1096.0 keV level.

4.4.13 1139 keV Level

Gamma decays of this level were not observed with
sufficient intensity to allow useful distribution data to
be measured.

4.4.14   1205 keV Level

Figure 4.15 shows the angular distribution of the decay from the 1205 keV level to the spin 3/2 831 keV level, which allows an initial-state spin of 3/2 or 5/2.

Malan et al. suggest a spin and parity of $5/2^+$, but their experiments cannot definitely exclude the possibility of $3/2^+$ or 7/2.

4.4.15   1212 keV Level

The angular distribution of the decay from the 1212 keV level to the spin 3/2 500 keV level allows a spin of 3/2 or 5/2 for the initial state. Inclusion of the correlation data from the 1212 keV to 500 keV to ground cascade (figure 4.16) fixes the spin of the 1212 keV state at 5/2, in agreement with Malan et al., who suggest that the level has negative parity.

4.4.16   1289 keV Level

Useful angular distribution or correlation data could not be obtained from the gamma decays of this level.

4.4.17   1298 keV Level

The angular distribution of the transition to the ground state (figure 4.17) allows a spin of ½ or 3/2 for the 1298 keV level, at the .1% confidence limit, with a clear preference for 3/2. Malan et al. assign $3/2^-$.

4.5 Mixing Ratios

Table 4.4 summarizes the mixing ratios (δ) of the gamma decays studied in the present work. The sign convention of Rose and Brink(1967) is used. The table also lists the results of Malan et al. (1974), which have been converted to the same sign convention.

When the parity of the initial state in ^{71}Ge is uncertain, Malan et al. give the mixing ratio determined for both initial parities. The two values are generally different because the population parameters of the state formed in ^{71}Ge (in the ^{71}Ga(p,nγ)^{71}Ge reaction) depend on the parity of the state. The distinction between the two possibilities is not made in the present work (^{68}Zn(α,nγ)^{71}Ge) because the variations permitted in the calculated population parameters in fitting the data overlapped the parameters determined for both parities.

TABLE 4.1

The branching ratios of the gamma decays of the
levels of ^{71}Ge, determined in the present experiment,
compared with those determined by Malan et al (1974).

Initial Level Energy	Final Level Energy	Branching Ratios (%)	
		Present Work	Malan et al.
525	175	11.8+0.5	10.6+0.6
	198	88.2+0.5	89.4+0.6
708	0	95.5+0.8	97.2+0.2
	175	4.5+0.8	2.8+0.2
747	0	24.8+1.1	22.3+0.8
	175	45.4+1.8	42.1+1.6
	500	29.8+2.4	35.6+2.0
808	0	43.6+1.6	43.4+1.4
	175	23.6+1.4	21.0+0.8
	500	32.8+1.5	35.6+1.6
831	0	66.3+1.4	64.1+1.4
	500	13.3+1.0	16.0+1.4
	525	18.9+1.2	18.3+1.2
	590	1.5+0.2	1.6+0.2
1027	0	<21.0+2.2	19.5+0.8
	175	<17.0+2.5	12.9+0.6
	500	<62.0+2.6	55.2+1.2
	747	obscured	12.4+0.8
1038	198	69.0+2.2	74.2+1.4
	590	31.0+2.2	25.8+1.4
1139	0	82.8+3.1	82.5+0.8
	175	10.1+2.6	10.3+0.6
	500	7.1+2.0	5.2+0.6
	708	<2	2.0+0.2
1205	525	9.9+3.0	10.3+1.2
	590	75.1+4.4	72.2+4.4
	831	15.0+2.6	17.5+5.4

Initial Level Energy	Final Level Energy	Branching Ratios (%) Present Work	Malan et'al.
1212	0	36.2+4.0	25.2+1.0
	175	17.1+3.6	21.5+2.2
	500	26.3+3.6	30.8+2.4
	708	11.2+4.5	14.4+4.2
	747	9.2+2.7	8.1+0.6

TABLE 4.2

The normalised coefficients of the Legendre

polynomial expansion of the gamma-ray

distributions, at 8.0 and 8.5 MeV bombarding

energy.

E_i	E_f	8MeV		8.5MeV	
		a_2	a_4	a_2	a_4
500	0	-0.08 ± 0.03	-0.02 ± 0.03	-0.10 ± 0.03	0.04 ± 0.02
525	175	0.23 ± 0.04	-0.14 ± 0.04	0.20 ± 0.03	0.00 ± 0.04
525	198	0.12 ± 0.02	-0.03 ± 0.03	0.09 ± 0.02	0.01 ± 0.02
590	198	0.15 ± 0.02	-0.02 ± 0.03	0.13 ± 0.02	0.02 ± 0.02
708	0	0.03 ± 0.03	-0.08 ± 0.05	0.01 ± 0.02	0.02 ± 0.02
708	175			0.06 ± 0.08	0.01 ± 0.09
747	0	0.42 ± 0.05	-0.17 ± 0.06	0.34 ± 0.03	0.01 ± 0.03
747	175	0.31 ± 0.03	-0.02 ± 0.04	0.26 ± 0.02	0.05 ± 0.03
747	500	-0.51 ± 0.03	0.02 ± 0.03	-0.43 ± 0.02	-0.02 ± 0.01
808	0	-0.03 ± 0.05	-0.02 ± 0.05	-0.07 ± 0.04	0.12 ± 0.05
808	175	0.09 ± 0.08	-0.24 ± 0.10		
808	500	-0.15 ± 0.03	0.03 ± 0.04	-0.08 ± 0.03	0.10 ± 0.06
831	0			-0.16 ± 0.03	-0.02 ± 0.03
831	500	0.14 ± 0.06	0.03 ± 0.07	0.10 ± 0.04	0.01 ± 0.05
831	525	-0.24 ± 0.03	-0.01 ± 0.04	-0.21 ± 0.02	-0.03 ± 0.02
1027	500	-0.65 ± 0.04	-0.05 ± 0.04	-0.63 ± 0.02	0.02 ± 0.02
1095.5 + 1096.0	175	-0.66 ± 0.06	0.17 ± 0.07	-0.63 ± 0.02	0.18 ± 0.03
1212	500			0.48 ± 0.08	0.04 ± 0.09
1298	0			-0.15 ± 0.04	-0.02 ± 0.04

TABLE 4.3

Normalised coefficients of the Legendre polynomial expansion of gamma-gamma correlations measured in the $^{68}Zn(\alpha,n\gamma\gamma)^{71}Ge$ reaction at $E_\alpha = 10$ MeV. The A1 geometry of the 747-500-0 cascade was not measured because of an electronic cut-off in one of the spectra.

Cascade	A1 Geometry		A2 Geometry	
	a_2	a_4	a_2	a_4
747-500-0	–	–	0.31 ± 0.06	-0.05 ± 0.07
808-500-0	-0.32 ± 0.10	0.02 ± 0.12	0.32 ± 0.10	0.08 ± 0.11
831-500-0	0.12 ± 0.10	0.17 ± 0.12	0.00 ± 0.20	0.03 ± 0.20
831-525-198	-0.14 ± 0.05	0.02 ± 0.06	-0.03 ± 0.05	0.01 ± 0.06
1026-500-0	-0.65 ± 0.04	0.03 ± 0.03	-0.30 ± 0.04	0.01 ± 0.04
1212-500-0	-0.48 ± 0.04	-0.06 ± 0.04	-0.23 ± 0.07	-0.12 ± 0.08

TABLE 4.4

A comparison of the mixing ratios (δ) obtained from the present work and the work of Malan et al. (1974). E_i and E_f are the energies in KeV of the initial and final nuclear levels, J_i and J_f are their angular momenta.

			Present Work		Malan et al.	
E_i	E_f	J_f	J_i	δ	J_i^π	δ
500	0	1/2	3/2	$-0.14^{+0.14}_{-0.09}$	$3/2^-$	-0.18 ± 0.20
				or 2.5 ± 0.8		or $2.75^{+3.56}_{-1.09}$
525	175	5/2	5/2	$-2.25^{+0.45}_{-0.65}$	$5/2^+$	$-2.05^{+0.45}_{-0.70}$
				or 0.21 ± 0.13		or $0.09^{+0.10}_{-0.11}$
590	198	9/2	7/2	0.23 ± 0.06	$7/2^+$	$0.18^{+0.03}_{-0.04}$
				or 3.1 ± 0.7		or $3.73^{+0.60}_{-0.46}$
					$7/2^-$	$0.16^{+0.03}_{-0.04}$
						or $3.73^{+0.60}_{-0.46}$
708	0	1/2	3/2	-0.27 ± 0.12	$3/2^-$	$0.19^{+0.08}_{-0.10}$
				or $3.7^{+2.6}_{-1.1}$		or $2.9^{+0.08}_{-0.76}$
747	175	5/2	5/2	-1.3 ± 0.4	$5/2^-$	$-2.05^{+0.32}_{-0.43}$
				or $0.0^{+0.14}_{-0.21}$		or 0.07 ± 0.07
747	500	3/2	5/2	$.27^{+1.87}_{-0.20}$	$5/2^-$	0.18 ± 0.07
						or $2.14^{+0.47}_{-0.34}$
808	500	3/2	1/2	$-2.75<\delta<-0.09$	$1/2^-$	unrestricted
831	0	1/2	3/2	$0.0^{+0.21}_{-0.16}$	$3/2^+$	$0.55^{+0.73}_{-0.41}$
				or $1.7^{+0.9}_{-0.6}$		
831	500	3/2	3/2	$\delta<0.2$	$3/2^+$	unrestricted
831	525	3/2	5/2	$\delta<-0.2$	$3/2^+$	unrestricted

			Present Work		Malan et al.	
E_i	E_f	J_f	J_i	δ	J_i^π	δ
1026	500	3/2	5/2	$0.45^{+0.66}_{-0.15}$	$5/2^-$	$0.73^{+0.65}_{-0.41}$
					$5/2^+$	$0.19^{+0.17}_{-1.29}$
						or $1.66^{+1.09}_{-1.39}$
1096	175	5/2	7/2	2.0 ± 0.3	$7/2^-$	$0.23^{+0.08}_{-0.07}$
						or $1.96^{+0.40}_{-0.30}$
					$7/2^+$	$0.32^{+0.17}_{-0.14}$
						or $1.66^{+0.70}_{-0.43}$
1205	831	3/2	3/2	$\delta>0.36$	$3/2^+$	$\delta>0.25$
		3/2	5/2	0.0 ± 0.14	$5/2^+$	0.0 ± 0.11
						or $3.08^{+1.62}_{-0.83}$
1212	500	3/2	5/2	$0.21^{+2.27}_{-0.09}$	$5/2^-$	$0.21^{+0.15}_{-0.14}$
						or $2.36^{+2.34}_{-0.76}$
1298	0	1/2	3/2	$0.12^{+0.18}_{-0.09}$	$3/2^-$	$-0.02^{+0.25}_{-0.19}$
				or $2.0^{+0.8}_{-0.6}$		Or $1.80^{+1.47}_{-0.73}$

FIGURE 4.1

The low-lying level scheme of ^{71}Ge with the gamma transitions observed in the ^{68}Zn$(\alpha, n\gamma)^{71}$Ge reaction.

1298.7
1288.6
1212.40
1209.03
1096.30
1095.55
1037.55
1026.5

831.2
808.1
747.2
708.1

589.5
525.1
499.9

198.3
174.9

0

3/2,(1/2)
5/2
3/2,5/2
7/2
5/2

3/2
1/2
5/2
1/2,3/2

5/2,7/2
5/2
3/2

9/2
5/2

1/2
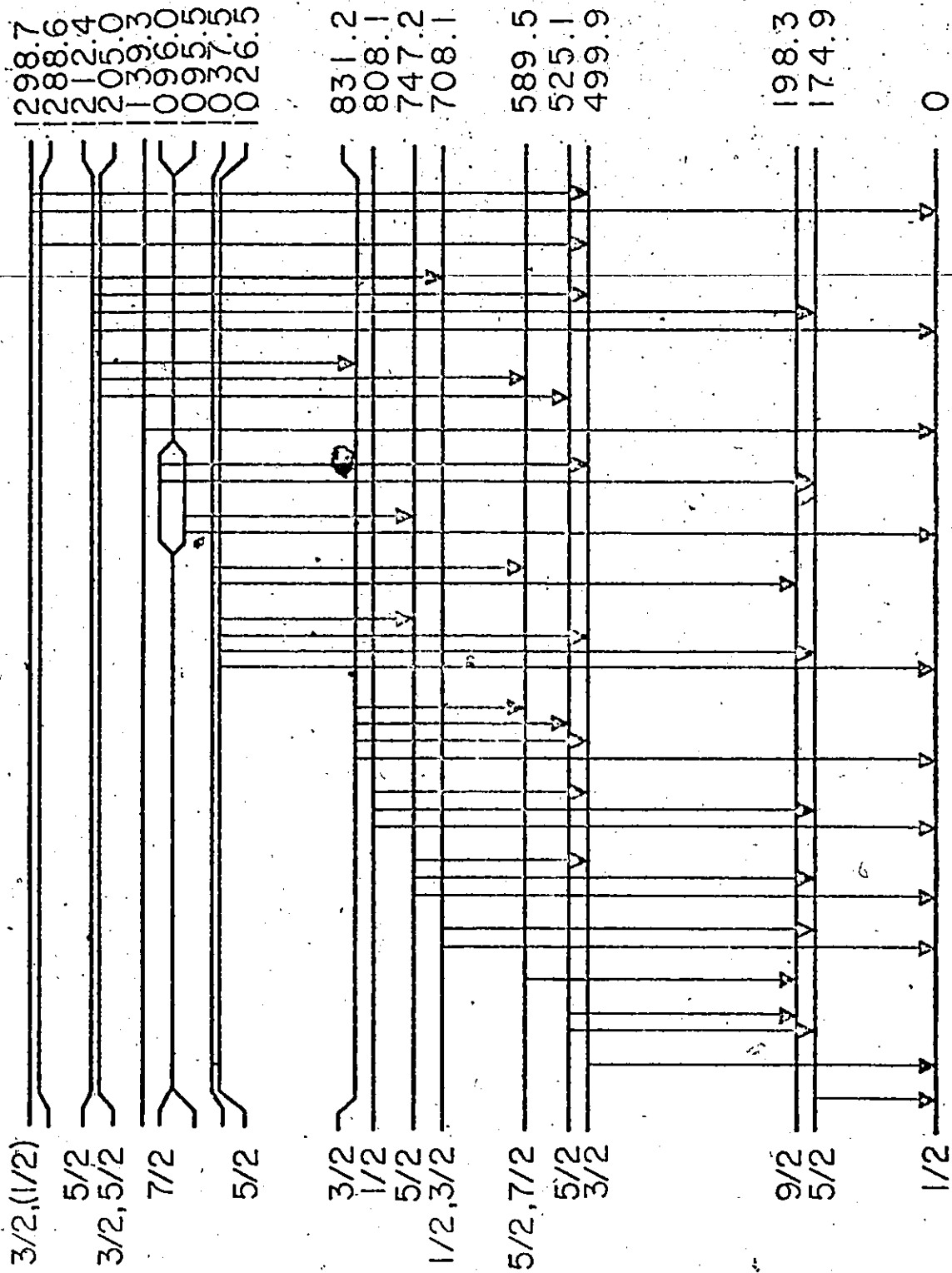
^{71}Ge

FIGURE 4.2

A spectrum of gamma rays from the $^{68}Zn(\alpha,n\gamma)^{71}Ge$
reaction, at an alpha bombarding energy of 8MeV,
collected by a 14cc Ge(Li) detector set at an
angle of 90° to the beam direction.

808-175
1205-590
747-175
^{197}Au
708-175
1026-500
1349-831
e$^+$e$^-$
500-0
^{23}Na (1543-1095)
^{26}Al
590-198
525-175
831-500
525-198
808-500
831-590
^{181}Ta
^{197}Au +1026-747
^{197}Au
747-500
^{197}Au
^{19}F
^{197}Au
175-0

1138-0
1095-0
^{68}Zn u
747-175
1095-175
831-0
808-0
1288-500
747-0
1212-500
708-0

Energy (keV)

10^6 10^5 10^4 10^3 10^2 10^1 10^0
10^6 10^5 10^4 10^3 10^2 10^1 10^0

200 300 400 500 600
700 800 900 1000 1100

FIGURE 4.3

A spectrum of gamma rays from the $^{68}Zn(\alpha,n\gamma\gamma)^{71}Ge$ reaction detected in the 65cc detector in coincidence with the 500 keV line in the 50cc detector, at an alpha bombarding energy of 10 MeV.
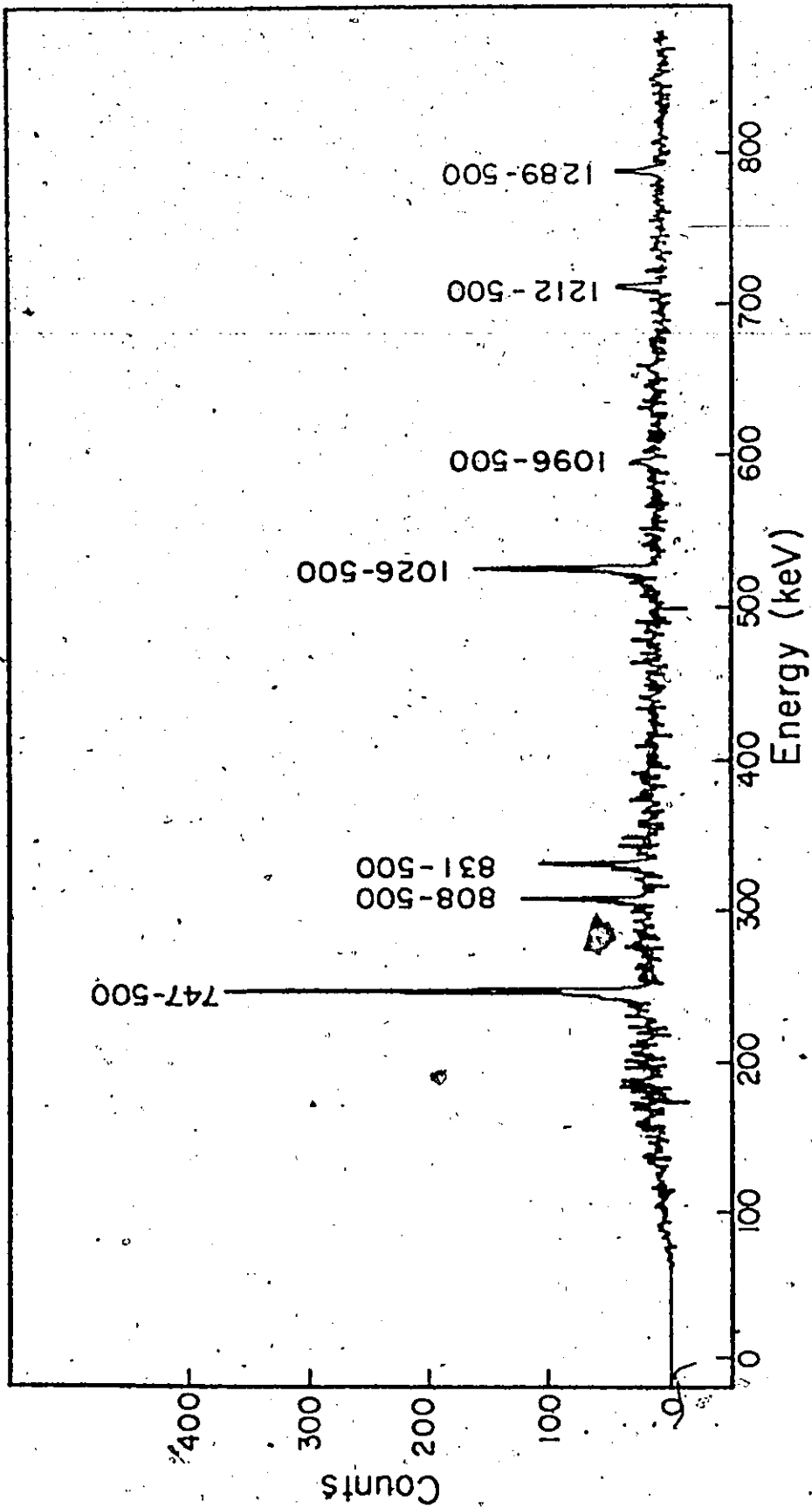
FIGURE 4.4

The angular distribution of the gamma transition from the 500 keV level in ^{71}Ge, populated in the ^{68}Zn$(\alpha, n\gamma)^{71}$Ge reaction at E_{α} = 8MeV, decaying to the spin $\frac{1}{2}$ ground state. Initial state spins of $\frac{1}{2}$, 3/2 and 5/2 are tested.

(a) Plots of χ^2 ($= S/\nu$) against arctan δ. The .1% confidence limit is indicated by the dashed line.

(b) The experimental distribution, with the best-fit theoretical lines for each different initial spin.
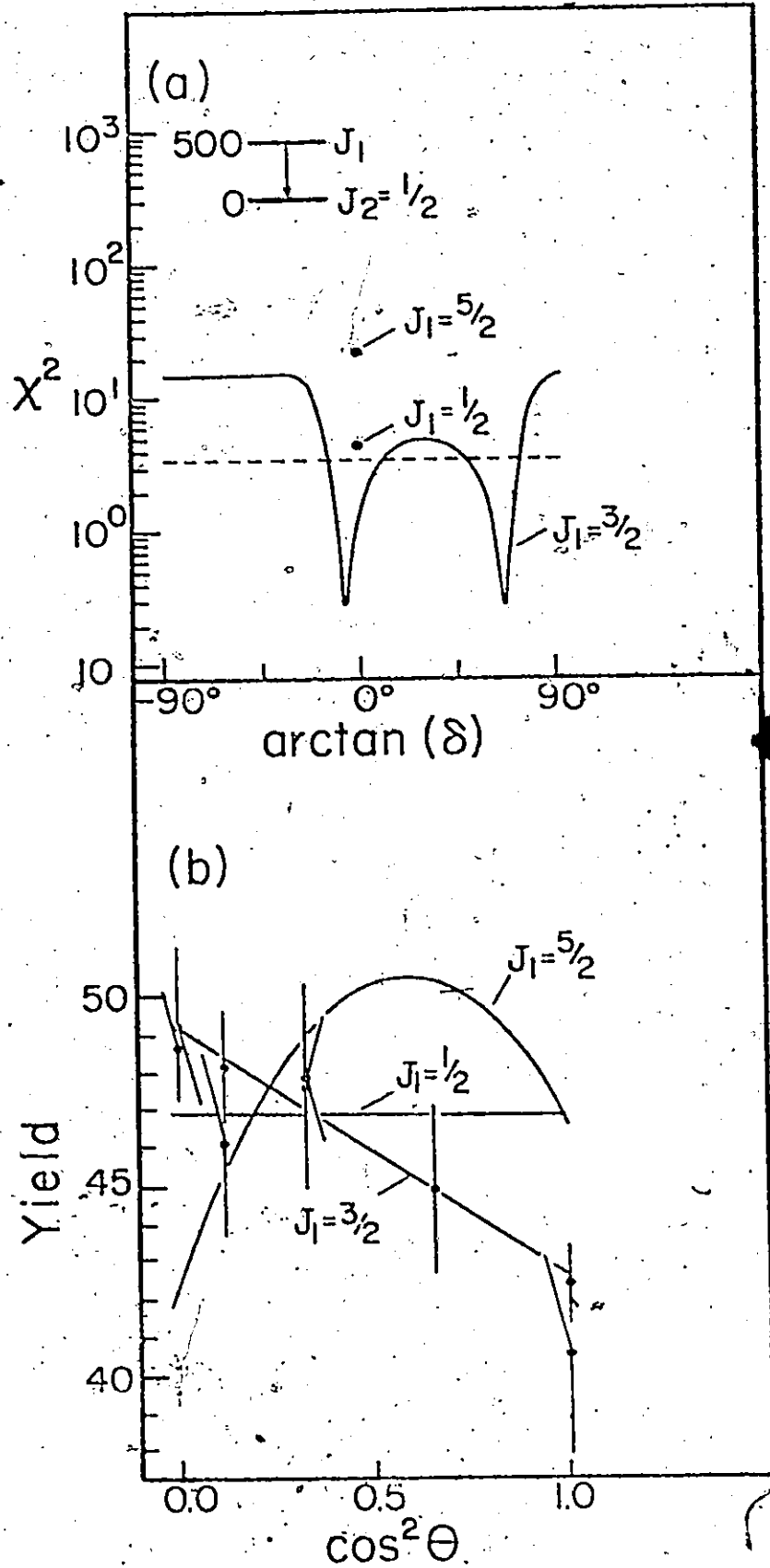
FIGURE 4.5

Angular distributions of the gamma transitions
from the 525 keV level, populated at $E_x = 8$ MeV,
to the spin 5/2 175 keV level and spin 9/2
198 keV level.

(a) 525 to 175 transition, χ^2 against arctan δ

(b) 525 to 175 transition, experimental and
best-fit theoretical distributions.

(c) 525 to 198 transition, χ^2 against arctan δ.

(d) 525 to 198 transition, experimental and
best-fit theoretical distributions.
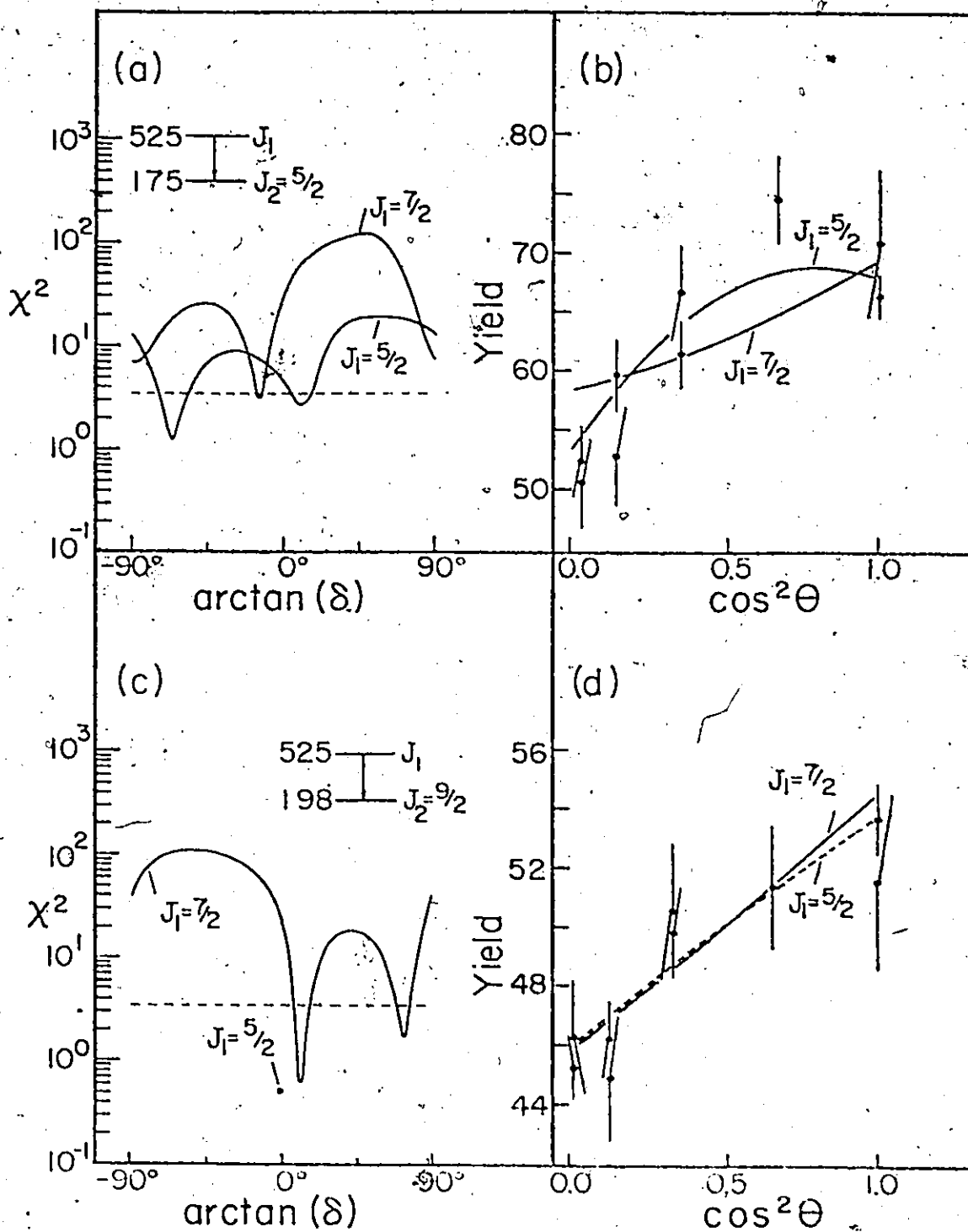
FIGURE 4.6

Angular distributions of the gamma transitions

from the 590 keV level to the spin 9/2 198 keV

level, and the 708 keV level to the spin ½

ground state, populated at E_α = 8MeV.

(a) 590 to 198 transition, χ^2 against arctan. δ.

(b) 590 to 198 transition, experimental and

best-fit theoretical distributions.

(c) 708 to ground state transition, χ^2 against

arctan δ.

(d) 708 to ground state transition, experimental

and best-fit theoretical distributions.

62
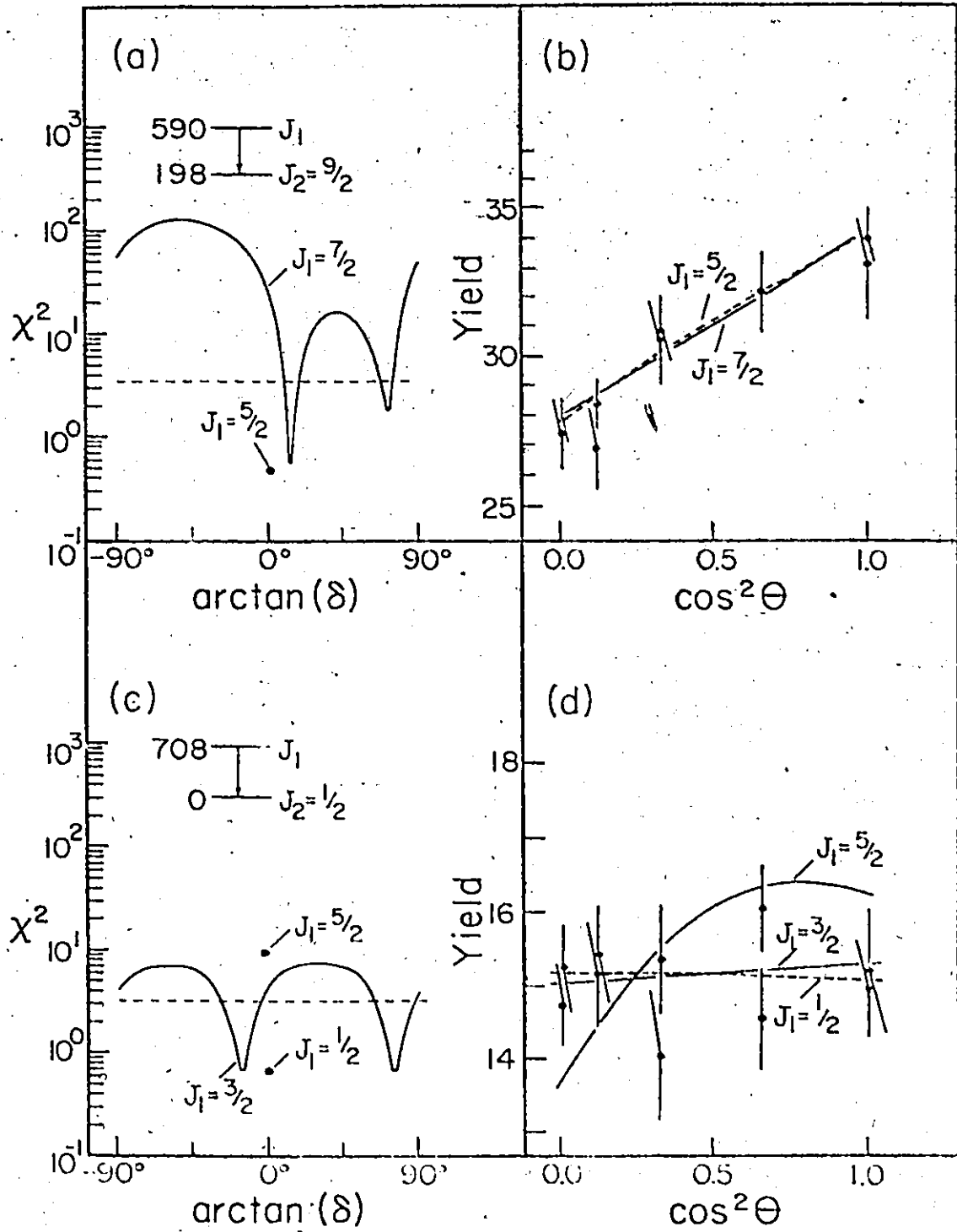
FIGURE 4.7

Angular distribution of gamma transitions
from the 747 keV level to the spin $\frac{1}{2}$ ground
state, and to the spin 5/2 level at 175 keV,
populated at $E_\alpha = 8MeV$.

(a) 747 to ground transition, χ^2 against
     arctan δ.

(b) 747 to ground transition, experimental
     and best-fit theoretical distributions.

(c) 747 to 175 transition, χ^2 against arctan δ.

(d) 747 to 175 transition, experimental and
     best-fit theoretical distributions.

(a)

χ^2

10^3

10^2

10^1

10^0

10^{-1}

747 ——— J_1

0 ——— $J_2 = 1/2$

$J_1 = 3/2$

$J_1 = 5/2$

-90°   0°   90°

arctan (δ)

(b)

Yield

40

35

30

25

20

15

$J_1 = 5/2$

$J_1 = 3/2$

$J_1 = 1/2$

0.0   0.5   1.0

$\cos^2\theta$

(c)

10^3

10^2

χ^2

10^1

10^0

10^{-1}

747 ——— J_1

175 ——— $J_2 = 5/2$

$J_1 = 3/2$

$J_1 = 1/2$

$J_1 = 5/2$

-90°   0°   90°

arctan (δ)

(d)

Yield

90

80

70

60

50

$J_1 = 5/2$

$J_1 = 3/2$

$J_1 = 1/2$

0.0   0.5   1.0

$\cos^2\theta$
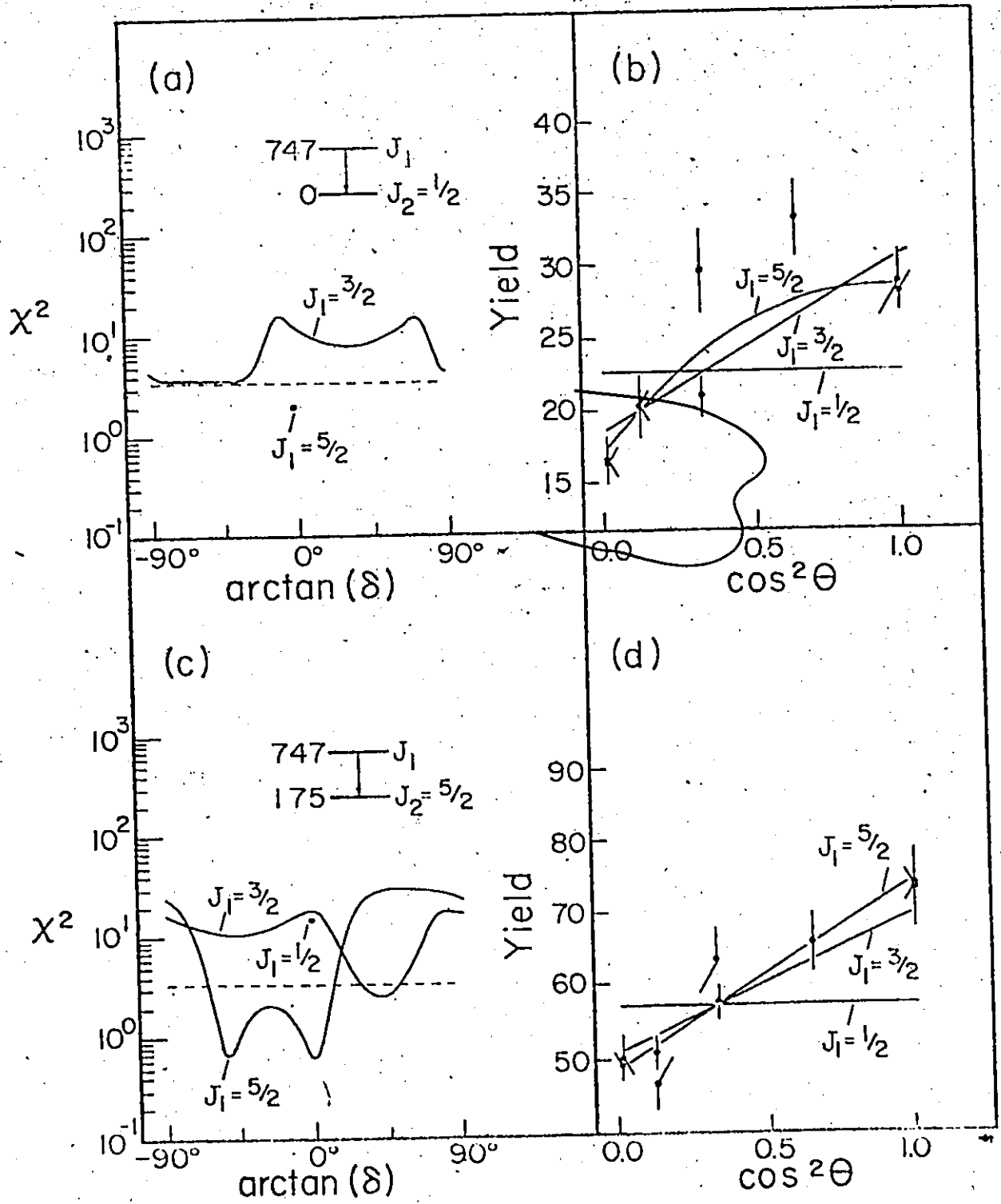
FIGURE 4.8

Angular distribution of the gamma transition

from the 747 keV level to the spin 3/2 level

at 500 keV, at E_α = 8MeV.

(a) χ^2 against arctan δ

(b) Experimental and best-fit theoretical

distributions.

FIGURE 4.9

Angular distributions of gamma transitions
from the 808 keV level to the spin $\frac{1}{2}$ ground
state and spin 5/2 175 keV state, at E_α = 8MeV.

(a) 808 to ground state, χ^2 against
     arctan δ.

(b) 808 to ground state, experimental and
     best-fit theoretical distributions.

(c) 808 to 175, χ^2 against arctan δ

(d) 808 to 175, experimental and best-fit
     theoretical distributions.
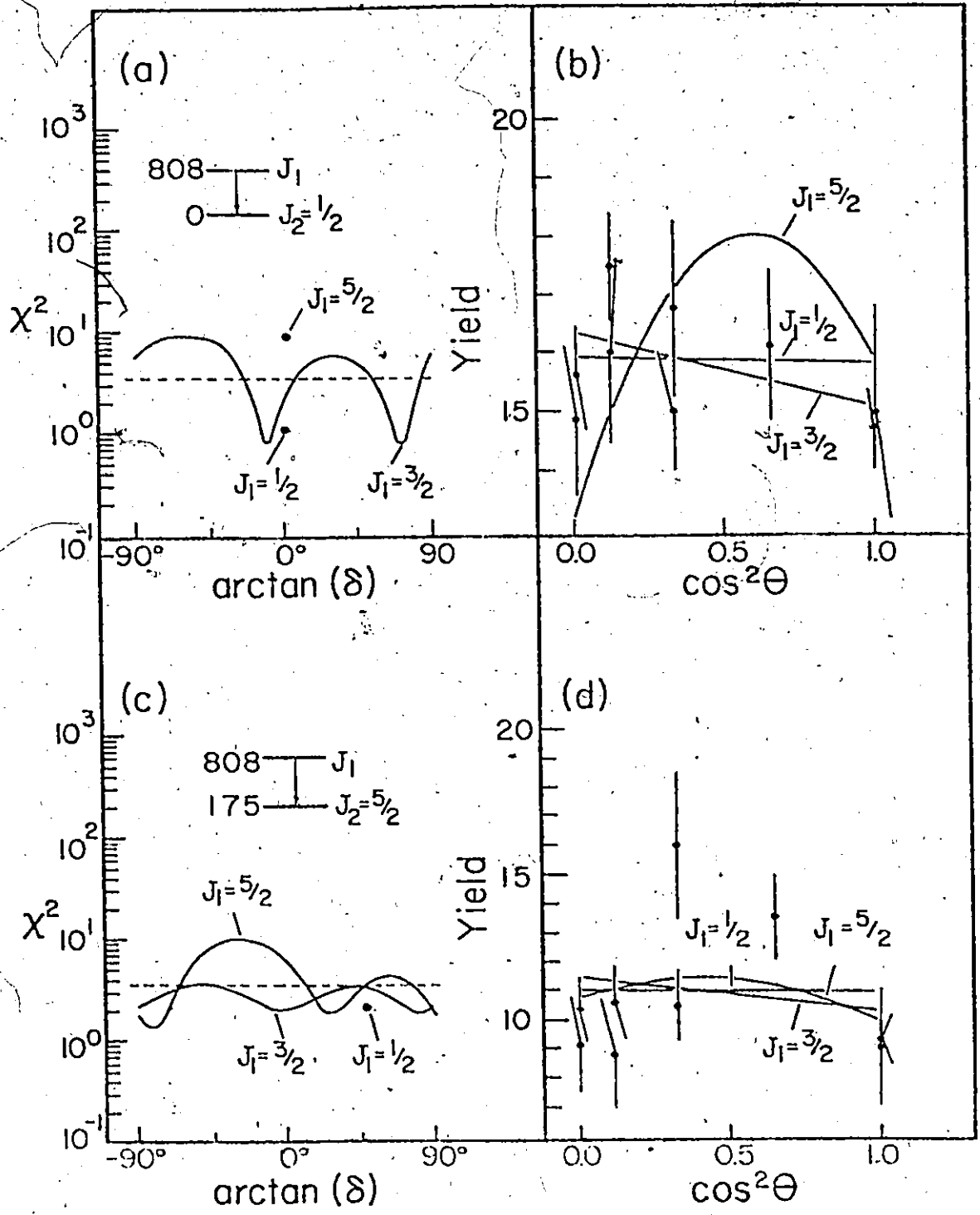
FIGURE 4.10

The angular distribution of the gamma transition
from the 808 keV level to the spin 3/2 500 keV
level, at E_α = 8 MeV, and A1 and A2 correlations
of the 808 to 500 to ground cascade, at $E\alpha$ = 10MeV.

(a) Total χ^2 of the angular distribution and
correlations, against arctan δ

(b) 808 to 500 transition, experimental and best-
fit theoretical distributions.

(c) 808-500-0, experimental and best-fit
theoretical correlations, A1 geometry.

(d) 808-500-0, experimental and best-fit
theoretical correlation, A2 geometry.

(a)

10^3

10^2

χ^2 10^1

10^0

10^{-1}

808 — J_1
500 — $J_2 = 3/2$
0 — $J_3 = 1/2$

$J_1 = 3/2$

$J_1 = 1/2$ $J_1 = 5/2$

$-90°$ $0°$ $90°$

arctan (δ)

(b)

60

Yield 50

40

$J_1 = 3/2$

$J_1 = 1/2$

$J_1 = 5/2$

0.0   0.5   1.0

$\cos^2 \Theta$

(c)

50

Yield 40

30

$J_1 = 3/2$

$J_1 = 5/2$

$J_1 = 1/2$

0.0   0.5   1.0

$\cos^2 \Theta$

(d)

50

Yield 40

30

$J_1 = 3/2$

$J_1 = 5/2$

$J_1 = 1/2$

0.0   0.5   1.0

$\cos^2 \Theta$
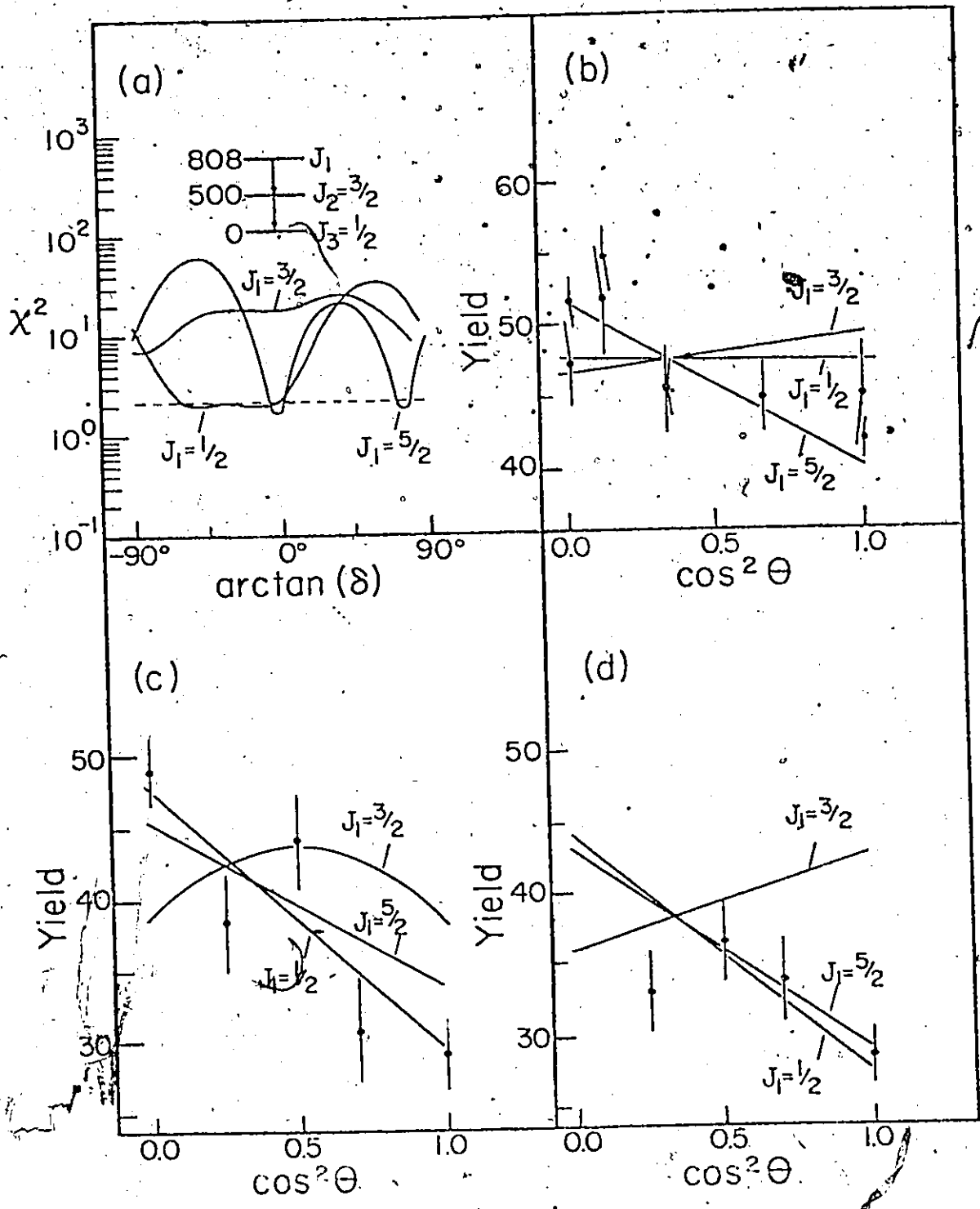
FIGURE 4.11

Angular distributions of gamma transitions from
the 831 keV level to the spin $\frac{1}{2}$ ground state,
and the spin 3/2 500 keV state, at $E\alpha = 8MeV$.

(a) 831 to ground state, χ^2 against arctan δ.

(b) 831 to ground state, experimental and
best-fit theoretical distributions.

(c) 831 to 500, χ^2 against arctan δ.

(d) 831 to 500, experimental and best-fit
theoretical distributions.
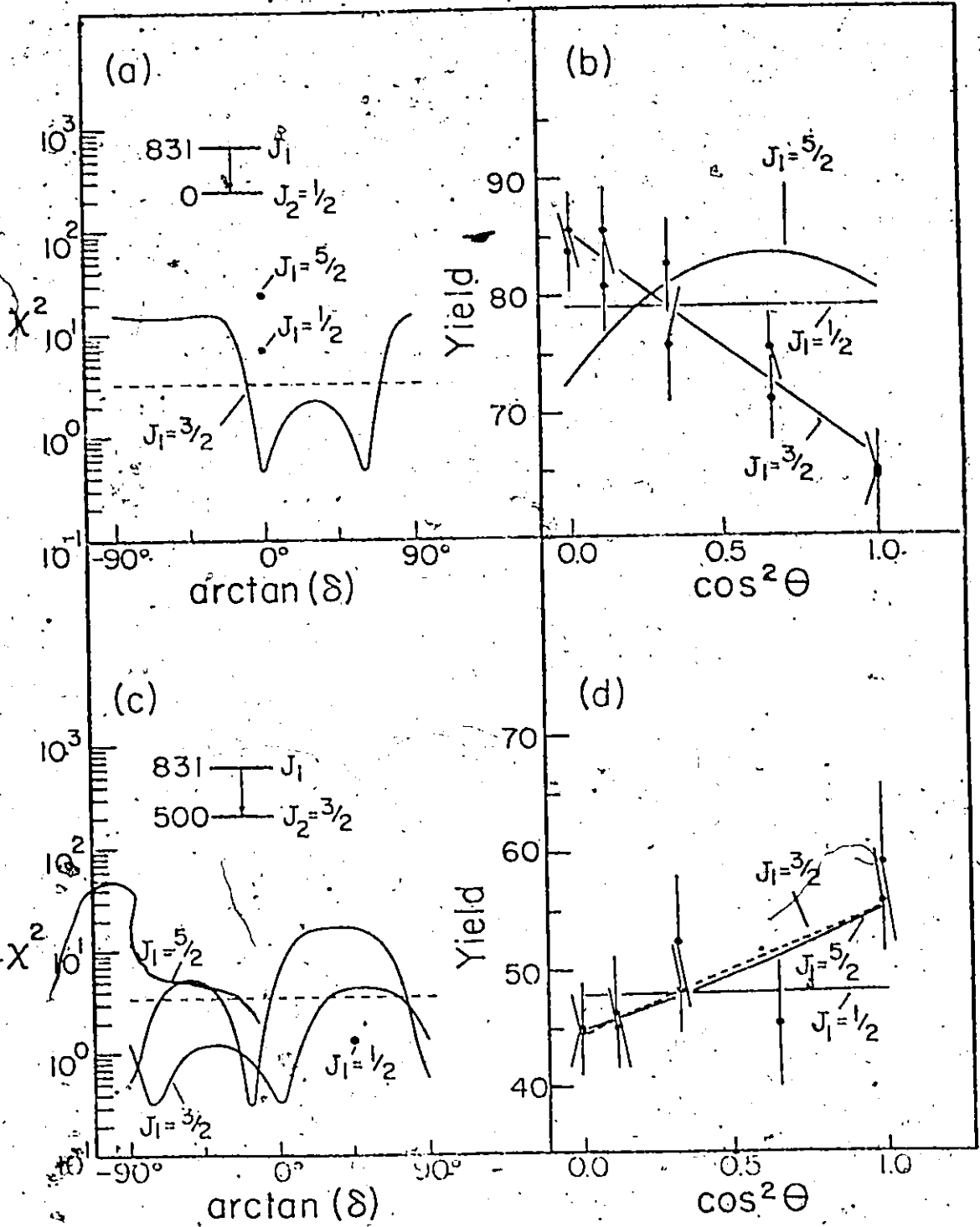
FIGURE 4.12

Angular distributions of gamma transitions from

the spin 3/2 831 keV level to the 525 and 590 keV

levels, at 8 MeV bombarding energy.

(a) 831 to 525, χ^2 against arctan δ.

(b) 831 to 525, experimental and best-fit

theoretical distributions.

(c) 831 to 590, χ^2 against arctan δ.

(d) 831 to 590, experimental and best-fit

theoretical distributions.
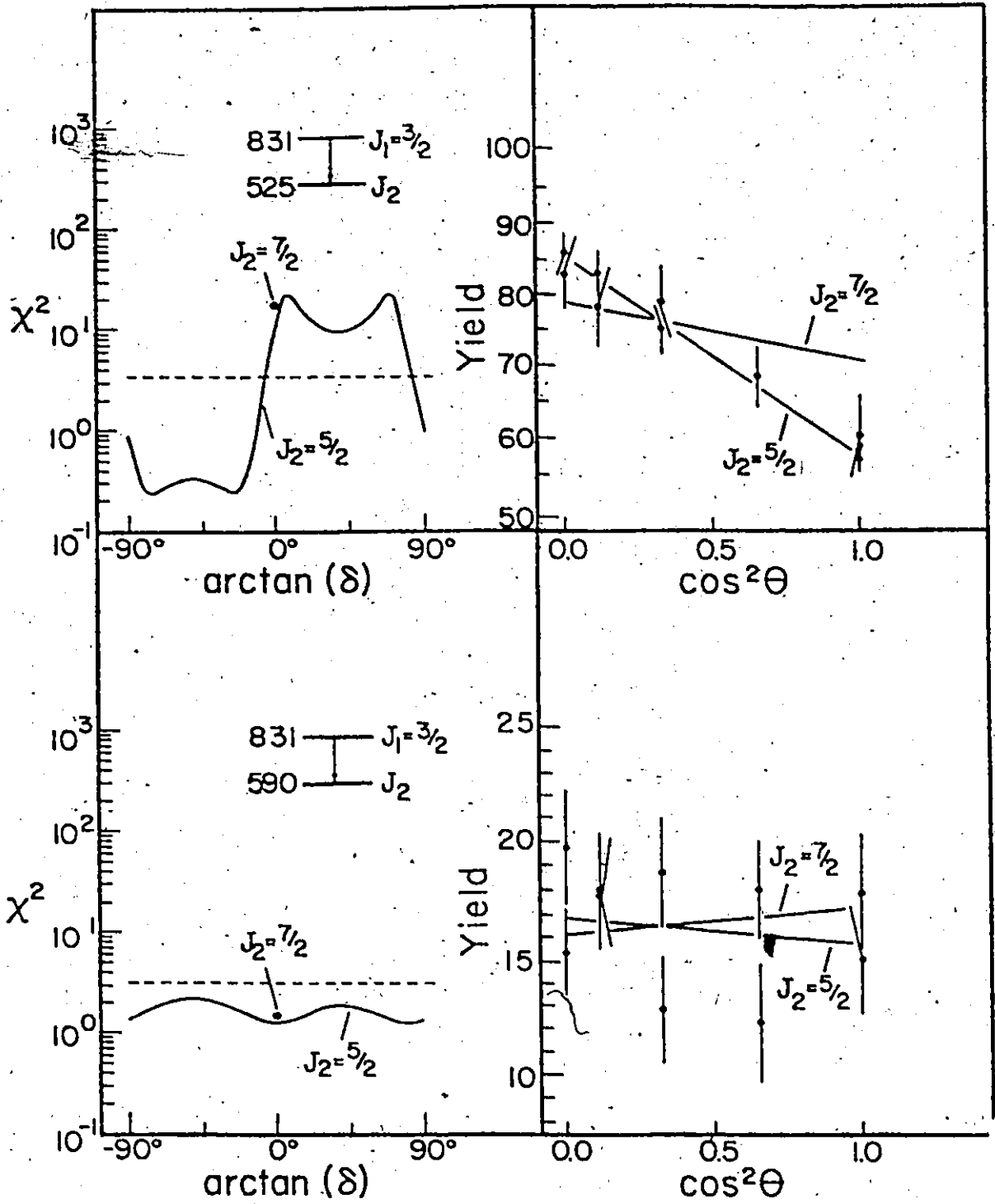
FIGURE 4.13

The angular distribution of the transition from the 1026 keV level to the spin 3/2 500 keV level, at $E_\alpha = 8$ MeV.

(a) χ^2 against arctan δ.

(b) Experimental and best-fit theoretical distributions.
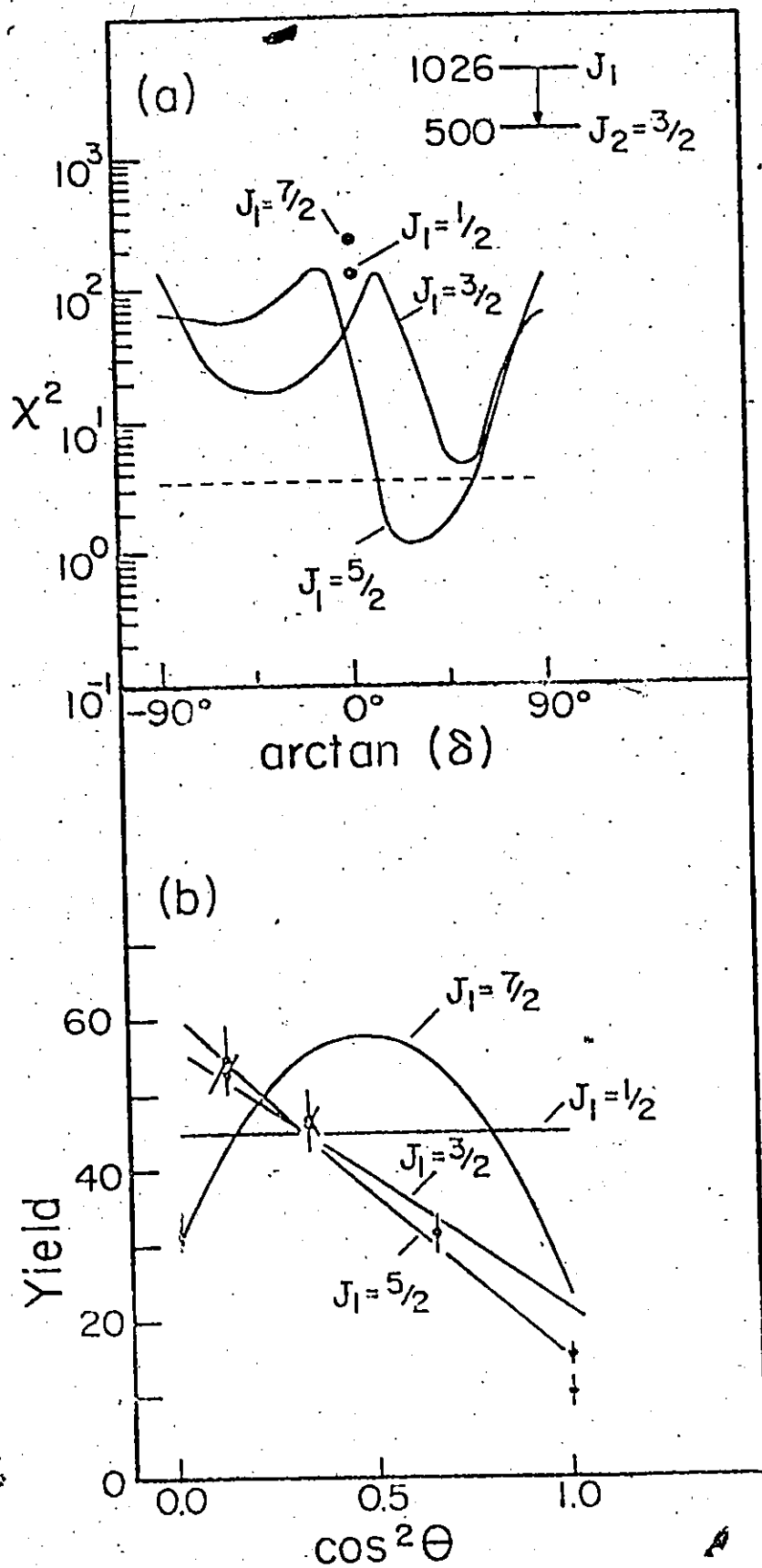
FIGURE 4.14

The angular distribution of the gamma transition from the 1096 keV level to the spin 5/2 175 keV level, at E_α = 8.5 MeV.

(a) χ^2 against arctan δ.

(b) Experimental and best-fit theoretical distributions.
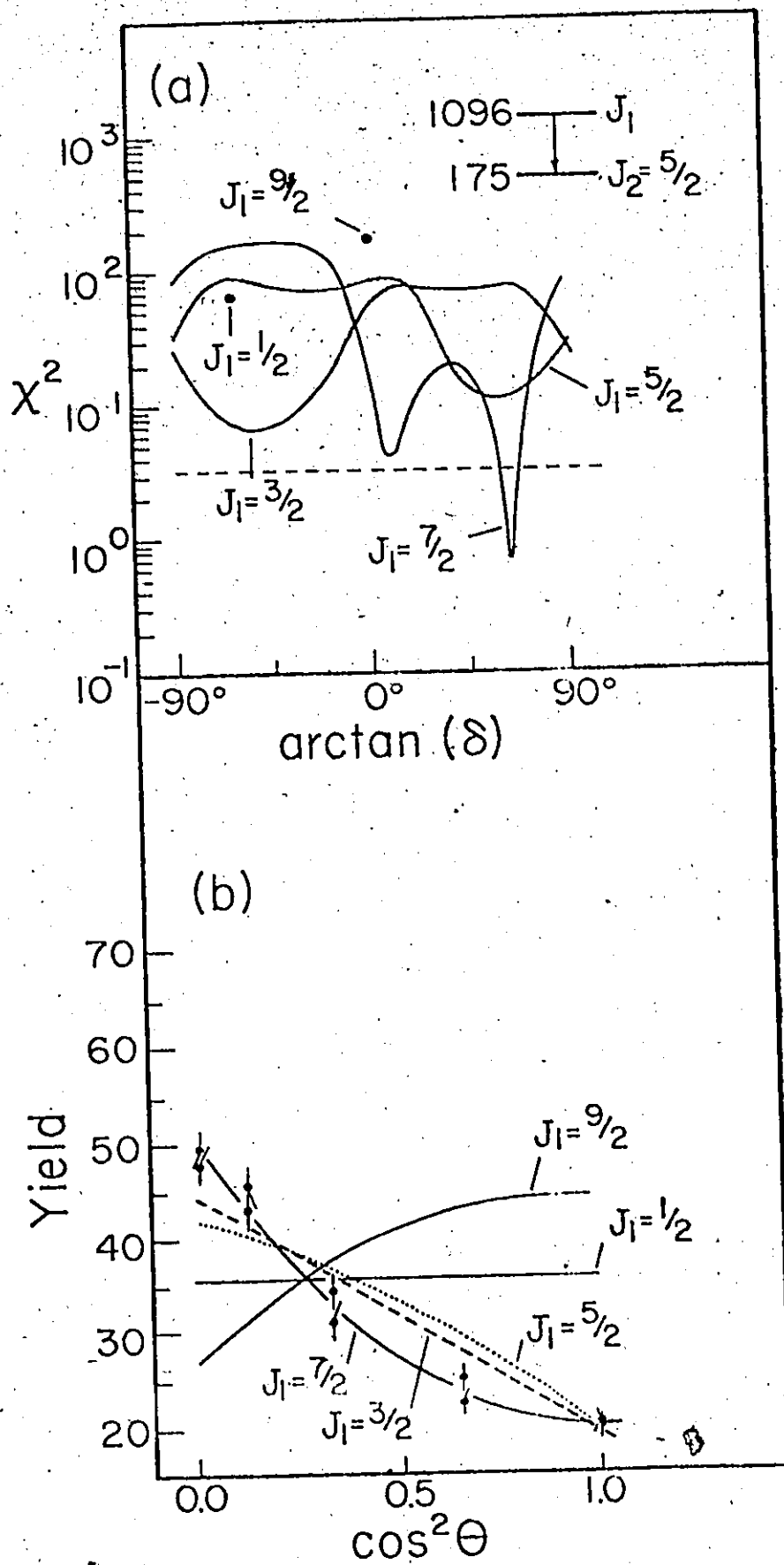
FIGURE 4.15

The angular distribution of the gamma transition
from the 1205 keV level to the spin 3/2 831 keV
level, at 8.5 MeV bombarding energy.

(a) χ^2 against arctan δ.

(b) Experimental and best-fit theoretical
distributions.
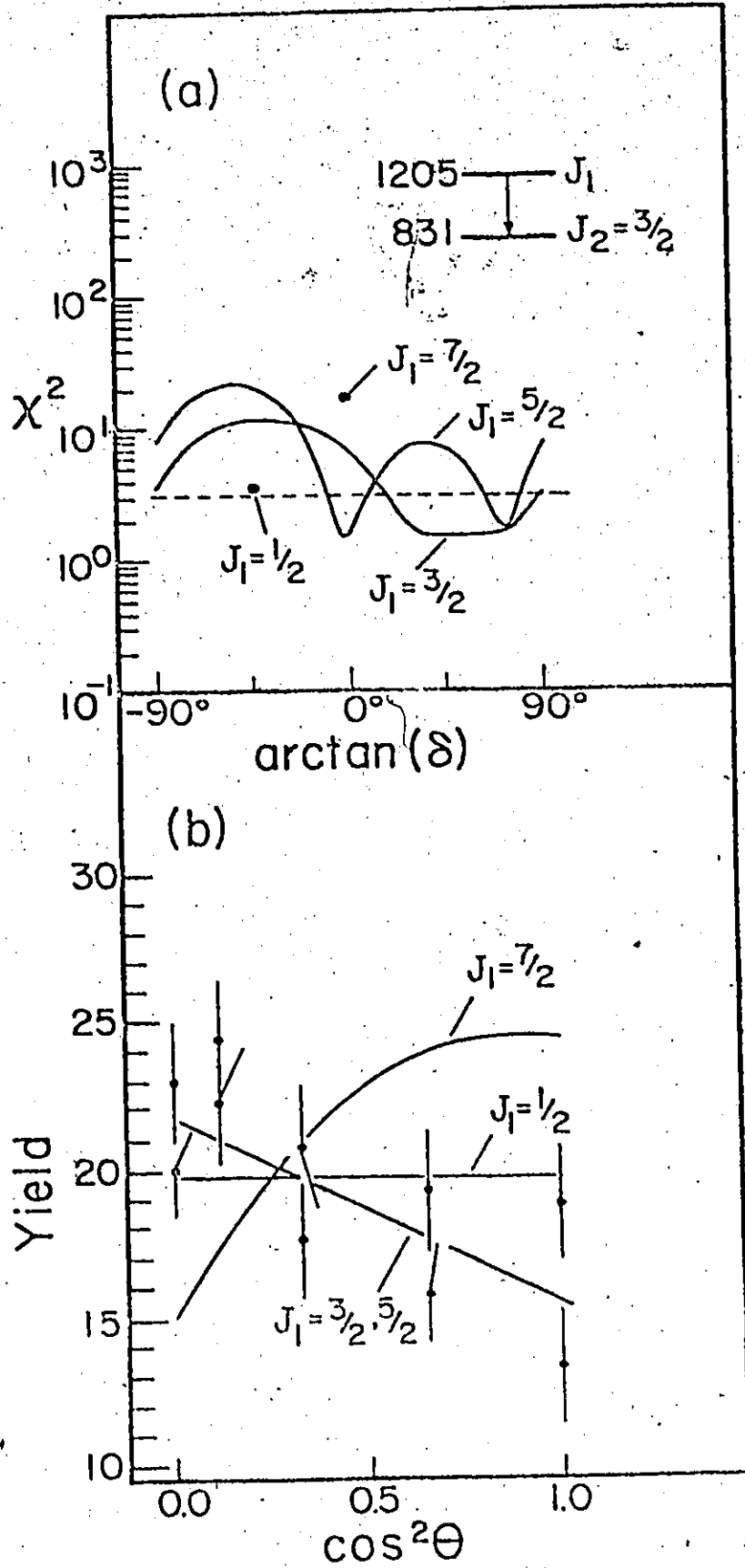
FIGURE 4.16

The angular distribution of the gamma transition
from the 1212 keV level to the spin 3/2 500 KeV
level, at E_α = 8.5 MeV, and A1 and A2 correlations
of the 1212 to 500 to ground cascade, at E_α = 10 MeV.

(a) Total χ^2 of the angular distribution and
   correlations, against arctan δ.

(b) 1212 to 500 transition, experimental and
   best-fit theoretical distributions.

(c) 1212-500-0, experimental and best-fit
   theoretical correlations, A1 geometry.

(d) 1212-500-0, experimental and best-fit
   theoretical correlations, A2 geometry.
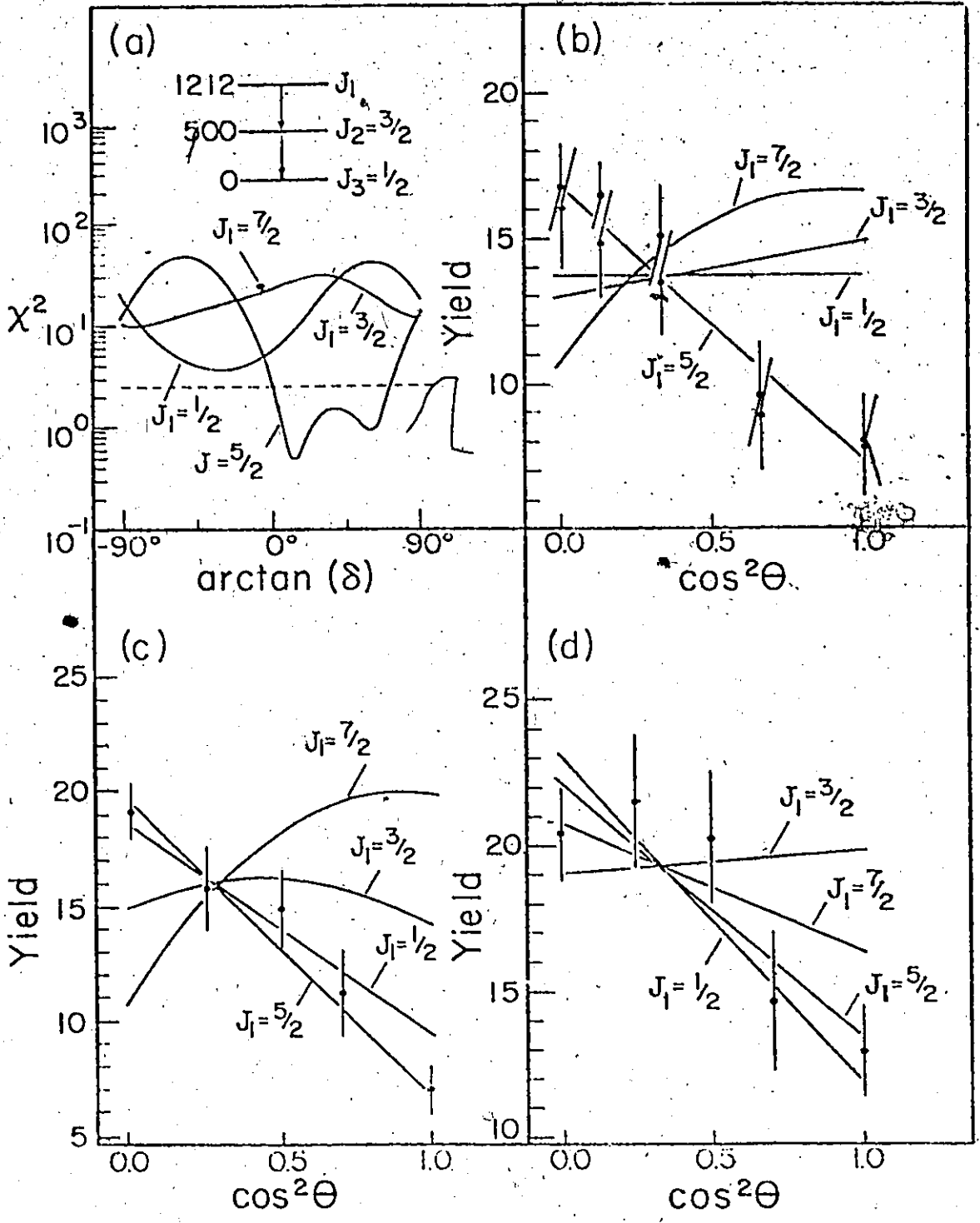
FIGURE 4.17

The angular distribution of the gamma transition

from the 1298 keV level to the spin $\frac{1}{2}$ ground state,

at $E\alpha = 8.5$ MeV.

(a) χ^2 against arctan δ.
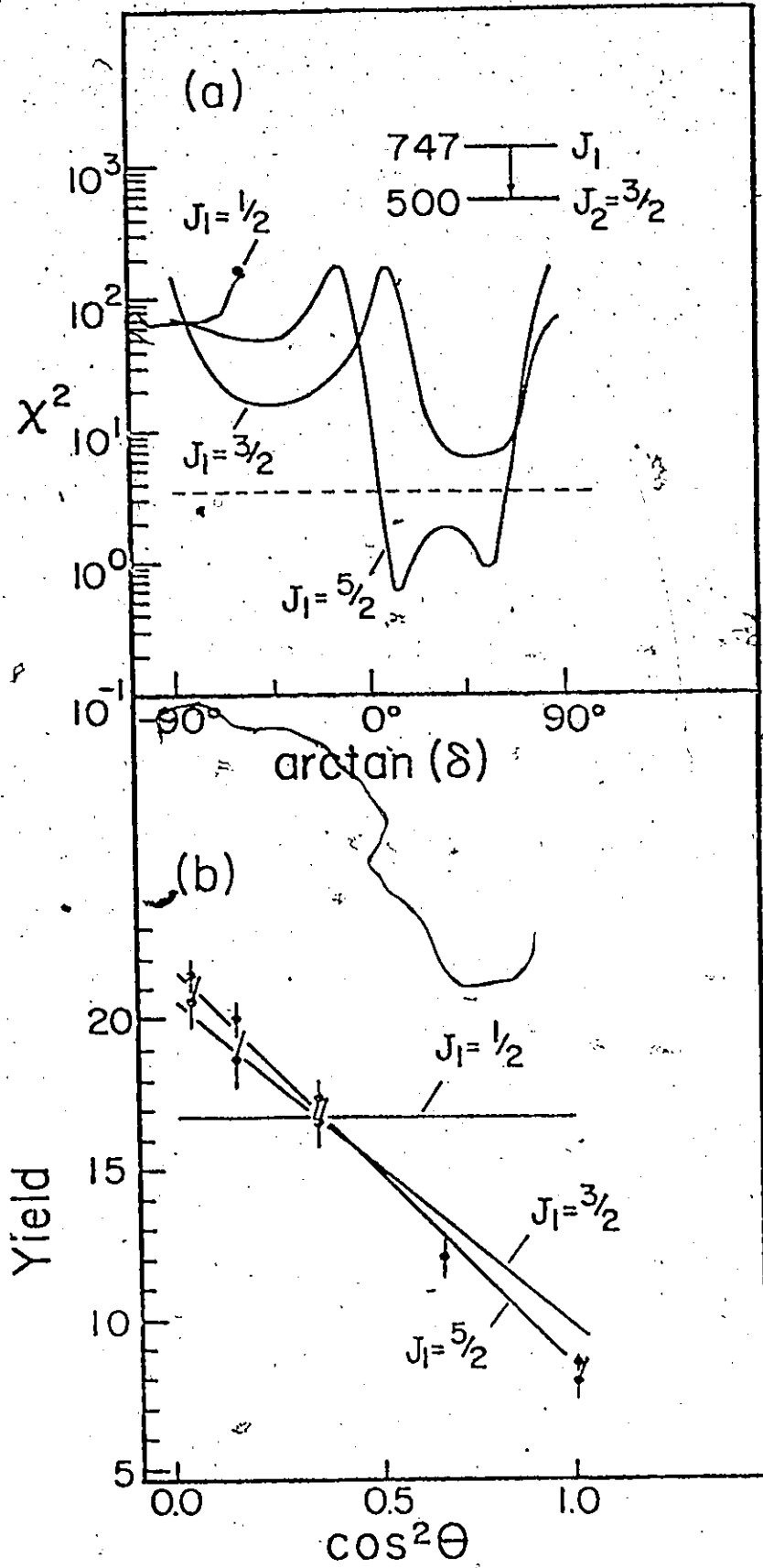
(b) Experimental and best-fit theoretical

distributions.

(a)

χ^2

$J_1 = 5/2$

$J_1 = 1/2$

$J_1 = 3/2$

arctan (δ)

(b)

Yield

$J_1 = 5/2$

$J_1 = 1/2$

$J_1 = 3/2$

$\cos^2\theta$
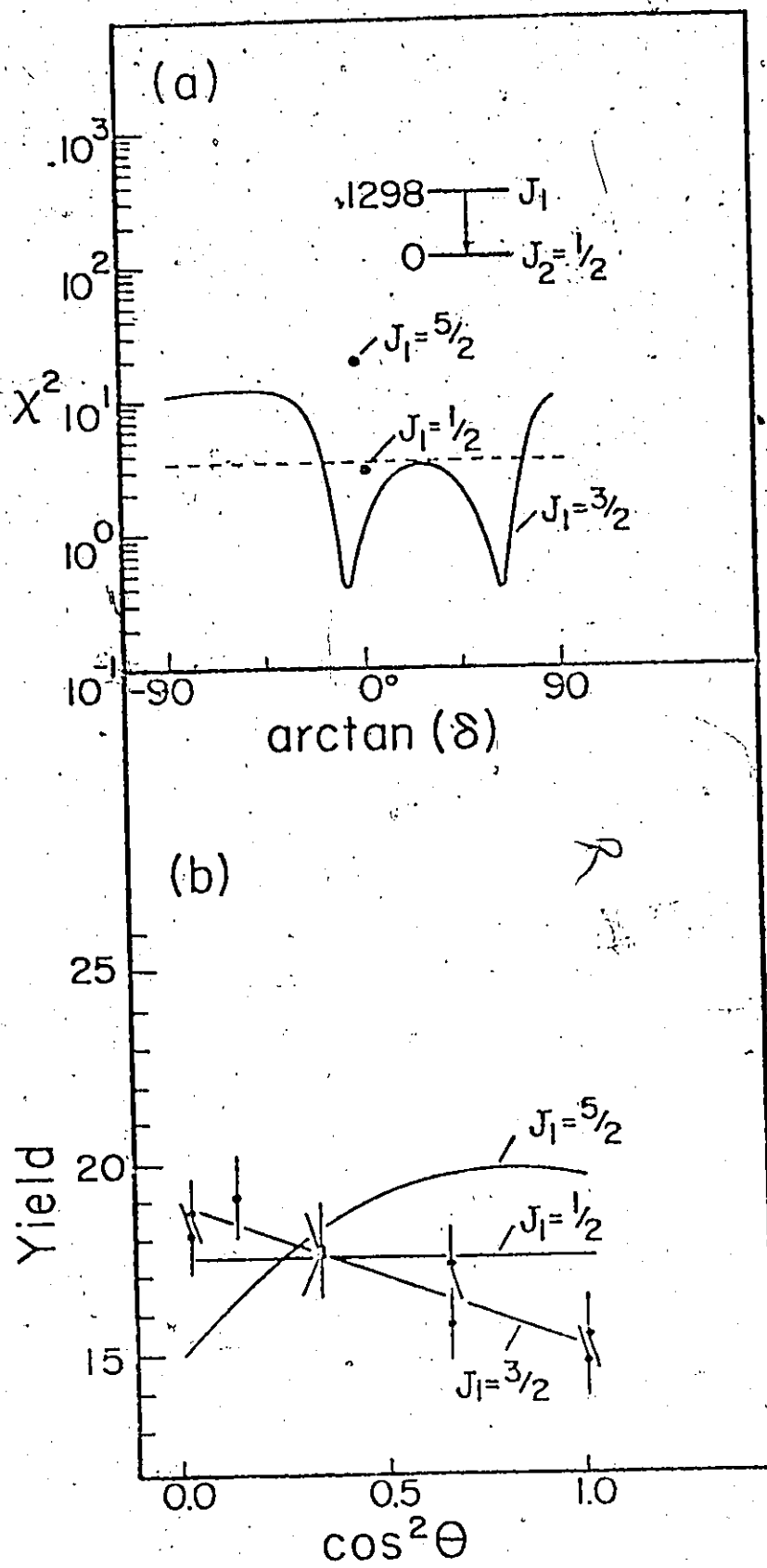
CHAPTER 5

THE INTERMEDIATE COUPLING MODEL

5.1 Introduction

As was pointed out in Chapter 1, a full shell-model description of the nucleus ^{71}Ge is difficult to calculate, so a description of the properties of ^{71}Ge is sought in terms of some simpler model. The excited states of the even-mass germanium isotopes show collective properties ; the gamma-ray transition strengths from excited states are several times the estimates given for single-particle transitions (Simpson et al. 1969), indicating that many particles are involved cooperatively in the excitations. If these collective excitations are stable structures, then it is plausible to attempt a description of the odd-mass germanium isotope ^{71}Ge in terms of the motion of the odd neutron moving in the potential provided by the doubly-even ^{70}Ge core. The ^{71}Ge ground state would consist of the ground state of ^{70}Ge coupled to the neutron in the single-particle orbital of lowest energy available; while excited states would be formed by promoting the neutron to a higher orbital, or exciting the core to one of its collective modes of excitation, or both.

The experiments of Forssten et al.(1974) lend support to this model of the odd germanium isotopes, since they have

located groups of high-spin levels in ^{69}Ge, ^{71}Ge and ^{73}Ge, which can be interpreted as being composed of a neutron in the $1g_{9/2}$ shell-model orbital, coupled to collective excitations of the relevant even-mass core.

The details of the interaction between the core and odd particle are determined by the nature of the core and its excitations. If the core is non-spherical the particle core interaction should be treated in the strong-coupling model, and the odd-particle wave-functions are based on Nilsson-model orbitals (Nilsson, 1955). If the average shape of the core is close to spherical, and the core excitations consist of collective oscillations around this average spherical shape, then the odd particle can be considered to be moving in a spherical shell-model potential, with perturbations due to the core oscillations, i.e. the weak or intermediate coupling model is appropriate.

The level spectra of the even-mass germanium isotopes (fig. 5.1) do not show well developed rotational structure, as expected of permanently deformed (i.e. non-spherical) nuclei, but rather show the features expected of quantised spherical liquid drops performing quadrupole oscillations, of the type described by Bohr (1952). In the ideal situation, where the oscillations are harmonic, the level spectrum of an even-even nucleus is expected to have a 0^+ ground state, a 2^+ first excited state, a 0^+, 2^+, 4^+ degenerate triplet at twice the energy of the first 2^+ state, etc. The low-lying

level structure of ^{74}Ge is reasonably close to the ideal model, but the level spectra of ^{70}Ge and ^{72}Ge deviate considerably from the model, the 0^+, 2^+, 4^+ triplet being widely split. However measurements of gamma-ray transition strengths in ^{70}Ge, and the quadrupole moment of the first excited state of ^{70}Ge (Simpson et al. 1969 and Simpson et al. 1972) are in good agreement with the predictions of the vibrational model.

The model of a particle coupled to the vibrations of a core was proposed by Bohr and Mottelson (1953), developed in the framework of the intermediate coupling model by Choudhury (1954), and has been extended and applied in numerous studies, e.g. Choudhury and O'Dwyer(1967), Glendenning (1960), Rustgi et al. (1968), Heyde and Brussard (1967) and Castel et al. (1971).

5.2 Development of the Model

In the intermediate coupling model the assumption is made that the Hamiltonian (H) describing the odd-mass (A+1) particle system can be split into two parts, thus:

$$H = H_c + H_{c-p} \qquad (5.1)$$

where H_c is the Hamiltonian of the even-even A-particle system, and H_{c-p} represents the interaction between the core and particle, taken to be a one-body potential. The

core Hamiltonian H_c is assumed to be described by the vibrational-collective model (Bohr, 1952), in which the core has, on the average, a spherical shape and undergoes surface vibrations.

In general the radius (R) of the nuclear surface of the core can be expressed in terms of the angular coordinates, Θ and ϕ, as:

$$R = R_0(1 + \sum_{\lambda=0}^{\infty} \sum_{\mu=-\lambda}^{+\lambda} \alpha_{\lambda\mu}^* Y_\lambda^\mu(\Theta,\phi) \qquad (5.2)$$

where R_0 is the average radius of the core, and the expansion coefficients $\alpha_{\lambda\mu}^*$ are time dependent, with average values of 0. The $\lambda = 0$ term corresponds to a 'breathing' mode of the nucleus, involving density vibrations of nuclear matter, and is not expected to be significant at low energies. The $\lambda = 1$ terms are also ignored since they correspond to motions of the centre-of-mass of the nucleus. The higher λ terms describe surface oscillations, whose energies, in the harmonic approximation, are given by:

$$E_{\lambda\mu} = \tfrac{1}{2}(B_\lambda^2 \mid \alpha_{\lambda\mu}\mid^2 + C_\lambda^2 \mid \dot{\alpha}_{\lambda\mu}\mid^2) \qquad (5.3)$$

where $\alpha_{\lambda\mu}$ is the time derivative of $\alpha_{\lambda\mu}$, and B_λ and C_λ are constants. The frequency of oscillation of each mode is given by:

$$\omega_\lambda = (\frac{C_\lambda}{B_\lambda}) \qquad (5.4)$$

In the quantised system each excitation (or phonon) of degree λ carries an energy $\hbar\omega_\lambda$, angular momentum λ, and has parity $(-)^\lambda$. Experimentally the lowest-lying states, in the region of interest, are interpreted as being built up from $\lambda = 2$ phonons, so higher degree excitations are ignored in the model, and the index λ is dropped from expressions describing the system.

The excitation energies of the spherical even-even nucleus undergoing quadrupole (i.e. $\lambda = 2$) surface oscillations are then given by $n\hbar\omega$, where n is the number of quadrupole phonons. Thus the first excited state, with angular momentum and parity 2^+, lies at $\hbar\omega$ above the 0^+ ground state, a 0^+, 2^+, 4^+ two-phonon triplet lies at $2\hbar\omega$, a 0^+, 2^+, 3^+, 4^+, 6^+ quintuplet lies at $3\hbar\omega$, etc.,

The interaction between the core and particle can now be determined. Suppose the spherical core provides an average spherical single-particle potential $V(r)$, then, if the equipotential lines of the core-particle interaction follow the shape of the surface of the core when it becomes distorted, the potential felt by the odd particle can be expressed, to first order in the deformation parameters as:

$$V(r,\theta,\phi) = V(r) - r\left(\frac{dV}{dr}\right)_{\alpha_\mu=0} \sum_\mu \alpha_\mu^* Y_2^\mu(\theta,\phi) \qquad (5.5)$$

Thus the total Hamiltonian of the core-plus-particle system can be written:

$$H = H_c + H_p + H_{int} \tag{5.6}$$

where H_c acts only on the quadrupole deformation coordinates of the core, H_p is a one-body spherically symmetric potential acting on the odd particle, and H_{int} couples the odd particle to the core vibrations through the interaction:

$$H_{int} = - k(r) \sum_\mu \alpha_\mu^* Y_2^\mu (\theta,\phi) \tag{5.7}$$

with $k(r) = r\frac{dV}{dr}$

The energies and wave functions of the combined system are then given by the eigenvalues (E) and eigenfunctions $|E;IM>$ satisfying:

$$H|E;IM> = E|E;IM> \tag{5.8}$$

where I and M are the angular momentum quantum numbers. The solutions to equation 5.8 can be expressed as sums of the solutions of the uncoupled Hamiltonian $H_c + H_p$, i.e.

$$|E;IM> = \sum_{NRn\ell j} C(NRn\ell j;I) \; |NRn\ell j;Im> \tag{5.9}$$

where $|NRn\ell_j;IM>$ is an eigenfunction of $H_c + H_p$, having angular momentum quantum numbers I and M. It is given by:

$$|NRn\ell j; IM\rangle = \sum_{\rho,m} (RJ\rho m|IM)|NR\rho\rangle |n\ell jm\rangle \qquad (5.10)$$

where $|NR\rho\rangle$ is the core eigenfunction, having N quadrupole

phonons, coupled to angular momentum R, projection ρ.

satisfying

$$H_c |NR\rho\rangle = (N + 5/2)\hbar\omega |NR\rho\rangle \qquad (5.11)$$

$|n\ell jm\rangle$ is the single-particle eigenfunction, of principal

quantum number n, orbital angular momentum ℓ, total angular

momentum j, having projection m, satisfying

$$H_p |n\ell jm\rangle = \varepsilon_{n\ell j} |n\ell jm\rangle \qquad (5.12)$$

where $\varepsilon_{n\ell j}$ is a shell-model single-particle energy.
The eigenvalues and eigenfunctions of the coupled system

are then found by diagonalising the matrix of H in the

uncoupled representation, i.e. the matrix whose elements are:

$$\langle N'R'n'\ell'j'; I'M'|H_c + H_p + H_{int}|NRn\ell j; IM\rangle \qquad (5.13)$$

These matrix elements are conveniently evaluated by changing

the coordinates describing the core oscillations from α_μ to

the phonon creation and annihilation operators $b_\mu^\dagger$ and b_μ,

defined by:

$$b_\mu = \frac{1}{(2B\hbar\omega)^{\frac{1}{2}}} (B\omega\, \alpha_\mu^\dagger + i\pi_\mu) \qquad (5.14)$$

$$b_\mu^\dagger = \frac{1}{(2B\hbar\omega)^{\frac{1}{2}}} (B\omega\, \alpha_\mu - i\pi_\mu^\dagger) \qquad$$

where π_μ is the momentum coordinate, conjugate to α_μ, defined by:

$$\pi_\mu = B\dot\alpha_\mu^\dagger \qquad (5.15)$$

The core Hamiltonian is then expressed:

$$H_c = \sum_\mu (b_\mu^\dagger b_\mu + \tfrac{1}{2})\hbar\omega \qquad (5.16)$$

and the interaction Hamiltonian is:

$$H_{int} = -k(r) \left(\frac{\hbar}{2B\omega}\right)^{\frac{1}{2}} \sum_\mu (b_\mu + (-)^\mu b_{-\mu}^\dagger)\, Y_2^{-\mu}(\theta,\phi) \qquad (5.17)$$

The operators $b_\mu^\dagger$ and b_μ have the property of increasing, or decreasing, by one the number of phonons in the core, when acting on the core wave-function.

The matrix element of H, given in the expression 5.13 then becomes:

$$N\hbar\omega\, \delta_{NN'}\, \delta_{RR'}\, \delta_{II'}\, \delta_{MM'} + \varepsilon_{n\ell j}\, \delta_{nn'}\, \delta_{\ell\ell'}\, \delta_{jj'}\, \delta_{II'}\, \delta_{MM'}$$

$$- \left(\frac{\hbar}{2B\omega}\right)^{\frac{1}{2}} \sum_{\mu} \sum_{\substack{\rho m \\ \rho'm'}} (Rj\rho m|IM)(R'j'\rho'm'|I'M') \langle n'\ell'|k(r)|n\ell \rangle$$

$$\times \langle j'm'|Y_2^\mu|jm \rangle \langle N'R'\rho'|b_\mu + (\text{-})^\mu b_{-\mu}^\dagger |NR\rho \rangle$$

The Wigner-Eckart theorem, according to the definition given by de Shalit and Talmi (1963), can be used on the matrix elements of the tensor operator Y_2^μ;

$$\langle j'm'|Y_2^\mu|jm \rangle = \frac{1}{\sqrt{2j'+1}}(j2m\mu|j'm')\langle j'||Y^2||j \rangle \qquad (5.19)$$

where the reduced matrix element $\langle j'||Y^2||j \rangle$ is given by:

$$\langle j'||Y^2||j \rangle = \left(\frac{5}{4\pi}\right)^{\frac{1}{2}} \sqrt{2j+1}\,(j2-\tfrac{1}{2}0|j'-\tfrac{1}{2})(1+(-)^{\ell+\ell'})/2$$

$$(5.20)$$

The operator $b_{-\mu}^\dagger$ is a tensor operator, so its matrix element can be expressed as:

$$\langle N'R'\rho'|b_{-\mu}^\dagger|NR\rho \rangle = \frac{1}{\sqrt{2R'+1}}(R2\rho-\mu|R'\rho')\langle N'R'||b^\dagger||NR \rangle$$

$$(5.21)$$

The operator b_μ is not a tensor operator, but its matrix element can be re-arranged to put it in terms of $b_\mu^\dagger$, and the Wigner-Eckart theorem can be applied (Choudhury, 1954).

The matrix element $\langle n'\ell'|k(r)|n\ell \rangle$ is only weakly dependent on n', ℓ', n and ℓ and is taken as a constant, k.

The interaction strength of H_{int} is expressed, for convenience, in terms of the dimensionless coupling constant ξ, defined by:

$$\xi = \left(\frac{5}{2\pi\hbar\omega C}\right)^{\frac{1}{2}} k \qquad (5.22)$$

The summation over the Clebsch-Gordan coefficients in the expression 5.18 can be performed, giving the contribution to the matrix element from the interaction H_{int} as;

$$-\left(\frac{\pi}{5}\right)^{\frac{1}{2}}\hbar\omega \, \xi \, (-)^{R'+j-I} \langle j'||Y^2||j\rangle \, \{\langle N'R'||b^\dagger||NR\rangle$$

$$+ (-)^{R'-R}\langle NR||b^\dagger||N'R'\rangle\}$$

$$\times W(R'j'Rj;I2) \, \delta_{II'}\delta_{MM'} \qquad (5.23)$$

The reduced matrix elements of $b^\dagger$ have been listed by Choudhury (1954), but must be multiplied by a factor $\sqrt{(2R+1)}$ because of a different definition used in the Wigner-Eckart theorem.

Thus the Hamiltonian matrix can be constructed for a given angular momentum I, and its projection M, within some restricted basis of the core and single particle states, if values of the phonon energy, $\hbar\omega$, the single particle energies $\varepsilon_{n\ell j}$, and the interaction strength ξ are chosen.

5.3 Modifications to the simple model

5.3.1. Pairing

The intermediate coupling model as developed in section 5.2 assumed that the core particles move in some average single-particle potential (or shell-model potential), with presumably some residual two-body (or many-body) interaction, which gives rise to the collectivity of the core excitations (Kisslinger and Sorensen, 1963). The model assumes that the core particles fill the shell-model orbitals, up to some well-defined maximum energy, and orbitals above this are completely empty, in the even-even nucleus, and are available to the odd particle in the odd-mass nucleus. However, there is a short-range component to the residual interaction between the core particles, acting most strongly between pairs of particles which have the same quantum numbers, except for the sign of their angular momentum projection quantum number m. This pairing interaction tends to scatter pairs of particles, in which the particles are coupled to a total angular momentum of zero, into the shell-model states which would be empty in the absence of the pairing force.

The problem of a system of particles interacting through a pairing force has been treated by Bardeen et al. (1957) in considering superconductors. The techniques that were developed were applied to the nuclear problem by Bohr et al. (1958).

When there is no residual interaction, the ground
state, $|\phi_o>$ of a system of particles obeying Fermi statistics,
in a one-body potential, is a product of the single-particle
wave functions, taken over all the single particle states up
to the highest occupied orbital, i.e.

$$|\phi_o> = \prod_{jm} a^\dagger_{jm} |0> \qquad (5.24)$$

where $a^\dagger_{jm}$ is the operator which creates a particle in the
shell-model state $|jm>$, with angular momentum quantum numbers
j and m, when acting on the vacuum state $|0>$.

An approximate solution to the ground state wave-
function of a system with an even number of particles, in
which there exists an attractive interaction between particles
in the single-particle states $|jm>$ and $|j-m>$ is:

$$|\phi_o> = \prod_{j} \prod_{m>o} (U_j + V_j \, a^\dagger_{jm} \, a^\dagger_{j-m}) \, |0> \qquad (5.25)$$

i.e. the pairs of particles are distributed over the available
single particle states, with probability V_j^2 that an orbital
is occupied by a pair, or U_j^2 that it is empty. In the non-
interacting case $V_j^2 = 1$ up to the maximum occupied orbital,
and is zero above this, i.e. the Fermi surface is sharp. In
the pairing solution U_j^2 and V_j^2 are given by:

$$U_j^2 = \tfrac{1}{2}\{1 + \frac{\varepsilon_j - \lambda}{((\varepsilon_j - \lambda)^2 + \Delta^2)^{\frac{1}{2}}}\} \qquad (5.26)$$

$$\text{and } V_j^2 = 1 - U_j^2 \qquad (5.27)$$

where ε_j is the energy of the single-particle orbital in the absence of the pairing interaction. The parameter Δ, which gives the diffuseness of the Fermi surface, is related to the strength of the pairing interaction by:

$$\Delta = G \, \Sigma_j U_j V_j \qquad (5.28)$$

where G is the magnitude of the pairing matrix element.

The average Fermi level, λ, is chosen to give the correct total number of particles (N) in the system, i.e.

$$N = \Sigma \, 2V_j^2 \qquad (5.29)$$

Thus in the even-even A-particle nucleus the pairing interaction promotes pairs of particles into shell-model orbitals that would otherwise be empty in the ground state. In the neighbouring (A+1) - particle nucleus one single-particle orbital, $|jm\rangle$, is occupied by the odd particle, so this orbital is 'blocked' and is not available for

occupation by a pair. The U_j and V_j coefficients of the

other unblocked orbitals have to re-adjust. The (A+1)-

particle state is said to be a one quasi-particle excitation

of the ground state of the A-particle system, and has the

wave function:

$$|\Phi_{jm}> = |jm> \prod_{j\neq j} \prod_{m'>0} (U_j' + V_j' a_{jm'}^{\dagger} a_{j-m'}^{\dagger})|0> \quad (5.30)$$

The quasi-particle, with quantum numbers j and m,

has the properties of a particle to the extent that the

orbital $|jm>$ was unoccupied, and the properties of a hole to

the extent that it was occupied in the ground state of the

A-particle system.

Instead of the single-particle energies ϵ_j, the

excitations of the (A+1)-particle system, with pairing, are

given by the quasi-particle energies, E_j, where:

$$E_j = ((\epsilon_j-\lambda)^2 + \Delta^2)^{\frac{1}{2}} \quad (5.31)$$

When quasi-particles are used in place of single-particle

wave functions in the intermediate coupling model, the single

particle energies, ϵ_j, are replaced by the quasi-particle

energies, E_j, and the matrix elements of H_{int} between states

involving the quasi-particles $|\Phi_{j'm'}>$ and $|\Phi_{jm}>$ are given by

the expression 5.23, with a further multiplicative factor

$(U_j U_j' - V_j V_j')$, where U_j and V_j are the emptiness and fullness

coefficients of the j, m orbital in the even-even nucleus
(Castel et al., 1971)

5.3.2. Non-Harmonicity in the Core

Generally a vibrational even-even nucleus does not
have a low-lying level structure given exactly by the
harmonic quadrupole-vibration model; anharmonic terms usually
split the two-phonon triplet which is predicted to lie at
energy $2\hbar\omega$. This is particularly true in ^{70}Ge.

To a first approximation, the anharmonic effects can
be allowed for in the intermediate coupling model of an odd-
mass nucleus by taking the energy of the two-phonon excitation
of angular momentum J as $(2 + \eta_J)\hbar\omega$, rather than $2\hbar\omega$, where
η_J reproduces the experimentally observed splitting of the
two-phonon state in the corresponding even-even nucleus
(Castel et al., 1971)

5.4 Application of the Model to ^{70}Ge

The values of the parameter describing the core
vibrations, $\hbar\omega$, and the splitting of the two phonon triplet
were taken from the level spectrum of ^{70}Ge. The two-phonon
triplet is widely split, but its energy centroid at 1.94 MeV
is quite close to twice the energy of the first 2^+ state in ^{70}Ge
at 1.04 MeV.

In the absence of a pairing interaction in the ^{70}Ge
core, the shell-model neutron $2p_{3/2}$ and $1f_{5/2}$ orbitals are

full, while the $2p_{\frac{1}{2}}$ and $1g_{9/2}$ orbitals are the next available for the odd neutron in ^{71}Ge. With the existence of a residual interaction between the neutrons in the ^{70}Ge core, having a component with pairing properties, the $2p_{3/2}$ and $1f_{5/2}$ orbitals are not completely full, while the $2p_{\frac{1}{2}}$ and $1g_{9/2}$ orbitals are not completely empty. The energies of the quasi-particles in ^{71}Ge based on these orbitals, and the emptiness and fullness coefficients (U_j and V_j) of the orbitals in ^{70}Ge have been investigated by the neutron-transfer direct reactions ^{70}Ge(d,p)^{71}Ge (Goldman, 1968), ^{70}Ge(p,d)^{69}Ge (Hsu et al., 1972) and ^{72}Ge(p,d)^{71}Ge (Fournier et al., 1972). The two sets of determinations, from the (p,d) pick-up reactions and (d,p) stripping reaction are compared in table 5.1. The agreement between the two determinations of the quasi-particle energies is poor. The results quoted by Fournier et al. are closer to the values expected in the mass region, so the occupation probabilities and single quasi-particle energies used in the intermediate-coupling model calculations were taken from the (p,d) data.

Having numerical estimates for the core parameters, and the particle parameters; the only remaining unknown required in the intermediate coupling calculation is the magnitude of the core-vibration-to-particle coupling parameter ξ. This can be estimated from the definition of $k(r)$ in equation 5. 7, in terms of the shell-model potential $V(r)$, which gives an estimate for $k = \langle n'\ell'|k(r)|n\ell \rangle$ as about 40 MeV

(Hecht, 1964). The parameter C in equation 5.22 depends on the 'surface tension' of the nuclear surface, and its magnitude can be estimated approximately from the liquid-drop model of the nucleus (Bohr and Mottelson, 1953) as about 60 MeV. Measurements of coulomb excitation (Temmer and Hydenburg, 1956) give C as being about 90 MeV in ^{70}Ge.

Taking C to be 90 MeV, and $\hbar\omega$ of the core to be 1 MeV, equation 5.22 gives ξ to be about 4.

A calculation of the positions of the negative and positive parity levels in ^{71}Ge, using the model of a neutron coupled to the quadrupole vibrations of the ^{70}Ge core is shown in figures 5.2 and 5.3. Core excitations including up to three phonons, and single quasi-particle states derived from the $2p_{\frac{1}{2}}$, $2p_{3/2}$, $1f_{5/2}$ and $1g_{9/2}$ orbitals were included in the calculation. The behaviour of the level scheme, with the lowest $\frac{1}{2}^{-}$ state taken at 0 MeV excitation, is shown as a function of the coupling parameter ξ, taken from 0 to 5. Figure 5.4 shows a comparison between the predicted level scheme of ^{71}Ge, with $\xi = 4$, and the level scheme deduced from the present work, the compilation given by Alvar (1973), the studies of Malan et al. (1974), and the studies of Forssten et al. (1974).

The lowest four calculated negative parity levels, having spins, $\frac{1}{2}$, 5/2, 3/2 and $\frac{1}{2}$ have obvious counterparts in the experimental level scheme, with the $\frac{1}{2}^{-}$ ground state, the 5/2^{-} 175 keV state, the 3/2^{-} 500 keV state and the spin $\frac{1}{2}$ 808 keV state, which is claimed to have negative parity by Malan

et al. The model calculation has less success with the positive parity states. The lowest $9/2^+$ state is depressed too far, relative to the lowest $\frac{1}{2}^-$ state, and the splitting of the $5/2^+$, $7/2^+$, $9/2^+$, $11/2^+$, $13/2^+$ multiplet based on coupling the $g_{9/2}$ quasi-particle to the one-phonon core state does not reproduce very well the ordering and spacing of the positive parity states believed to exist between 500 keV and 1100 keV. The presence of the state at 831 keV, in the experimental level scheme, with spin 3/2, and, according to Malan et al., with a preference for positive parity is particularly difficult to account for. In the framework of the model, the lowest $3/2^+$ state, based on coupling the $g_{9/2}$ quasi-particle to the two-phonon 4^+ core state, is above 2 MeV in excitation. The assignment of positive parity to the 831 keV state is based on the excitation intensity of the level in the $^{71}Ga(p,n\ \gamma)^{71}Ge$ reaction (Malan et al., 1974), and this assignment relies heavily on the applicability of the Compound Nucleus Statistical Reaction Model. According to the compilation of Alvar (1973), the positive parity assignment is contradicted by the observation of an $\ell = 1$ stripping pattern in a very weakly populated angular distribution in the $^{72}Ge(p,d)^{71}Ge$ reaction. Moreover, the recent measurements of Onizuka et al. (1975) on the rates of decay of the levels of ^{71}Ge by electron internal conversion prefer negative parity for the 831 keV level.

If the 831 keV level has negative parity then its presence is not so difficult to explain.

TABLE 5.1

Single quasi-particle energies (E_j) in ^{71}Ge and occupation probabilities (V_j^2) of orbitals in ^{70}Ge.
(a) Data from the ^{70}Ge$(d,p)^{71}$Ge reaction studied by Goldman (1968). The occupation probabilities have been re-normalised by Hsu et al. (1972).
(b) Data from the ^{70}Ge$(p,d)^{69}$Ge reaction (Hsu et al., 1972) and ^{72}Ge$(p,d)^{71}$Ge reaction (Fournier et al., 1973).

Orbital	(a) E_j	V_j^2	(b) E_j	V_j^2
$2p_{1/2}$	0.3	0.40	0.0	0.30-0.49
$2p_{3/2}$	2.0	0.96	0.84	0.69-0.80
$1f_{5/2}$	1.3	0.64	0.60	0.86
$1g_{9/2}$	0.2	0.16	0.19	0.10

FIGURE 5.1

The low-lying levels of the even-mass isotopes of
germanium.   The level schemes were taken from:

^{70}Ge: Hinrichsen,Van Patter and Shapiro (1969)

^{72}Ge: Camp (1968)

^{74}Ge: Camp, Fielder and Foster (1971)

^{76}Ge: Camp and Foster (1971)

FIGURE 5.1

106

FIGURE 5.1

Energy level diagrams for ^{70}Ge, ^{72}Ge, ^{74}Ge, and ^{76}Ge.

^{70}Ge:
- 4^+ —— 2153
- 2^+ —— 1708
- 0^+ —— 1216
- 2^+ —— 1040
- 0^+ —— ^{70}Ge

^{72}Ge:
- 4^+ —— 1728
- 2^+ —— 1464
- 2^+ —— 833
- 0^+ —— 691
- 0^+ —— ^{72}Ge

^{74}Ge:
- 0^+ —— 1482
- 4^+ —— 1464
- 2^+ —— 1204
- 2^+ —— 596
- 0^+ —— ^{74}Ge

^{76}Ge:
- 0^+ —— 1911
- (3^+) —— 1539
- 4^+ —— 1401
- 2^+ —— 1108
- 2^+ —— 562
- 0^+ —— ^{76}Ge

FIGURE 5.2

The negative-parity levels of ^{71}Ge in the intermediate-coupling model, as a function of the coupling strength ξ, relative to the lowest $\frac{1}{2}^-$ level, including up to 3-phonon core excitations and single quasi-particle excitations based on the $2p_{1/2}$, $2p_{3/2}$ and $1f_{5/2}$ orbitals.

Core parameters: $\hbar\omega = 1.040$

$\eta_0 = -0.831$

$\eta_2 = -0.356$

$\eta_4 = 0.070$

Particle Parameters:

Orbital	Quasi-Particle Energy(MeV)	U_j	V_j
$2p_{1/2}$	0.0	.774	.632
$2p_{3/2}$	0.84	.500	.866
$1f_{5/2}$	0.60	.374	.927
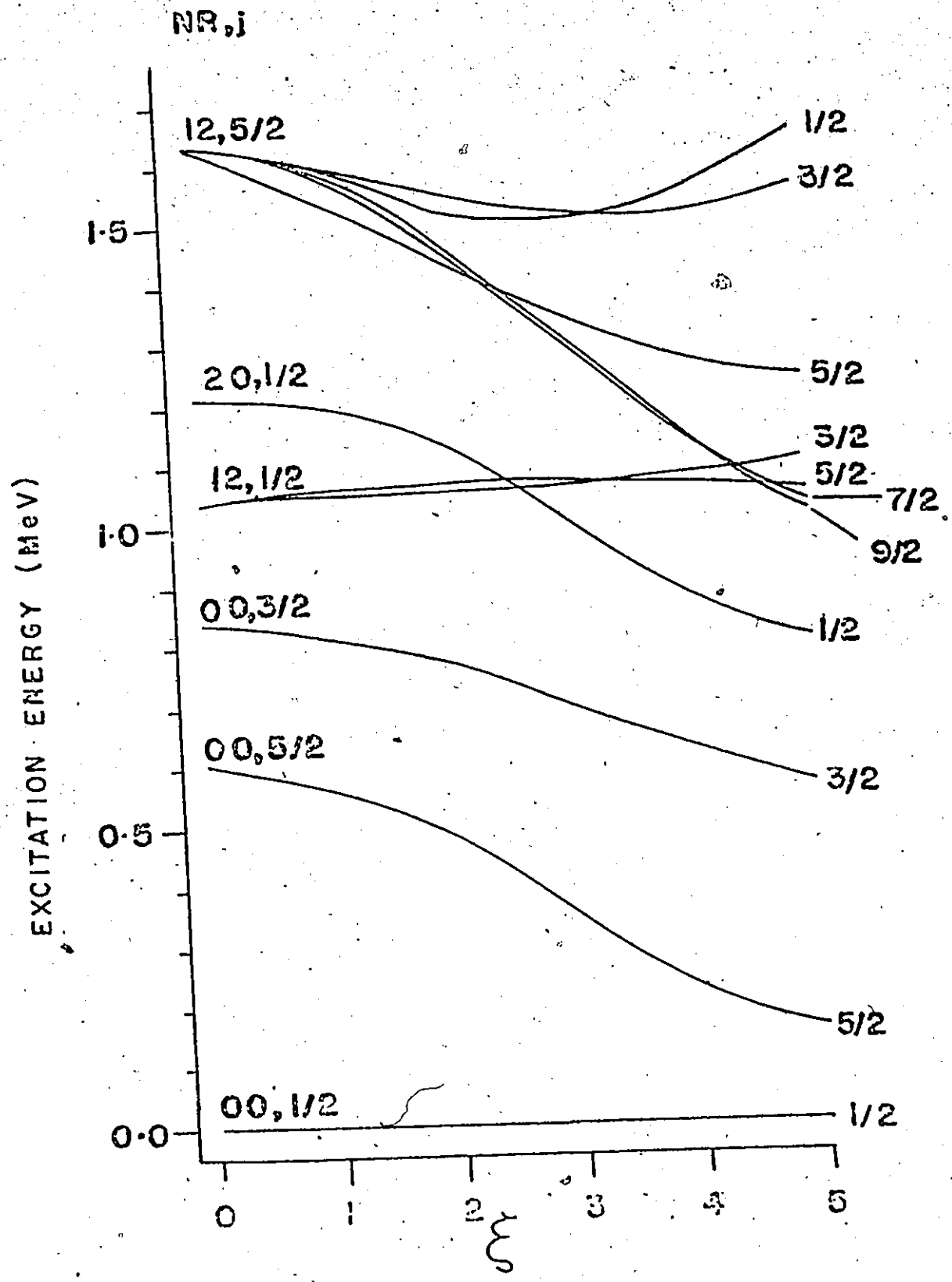
FIGURE 5.3

The positive-parity levels of ^{71}Ge in the intermediate
coupling model, relative to the lowest 1/2$^-$ level.
The core parameters are as in figure 5.2. The
parameters for the quasi-particle are:

Orbital	Quasi-particle Energy(MeV)	U_j	V_j
$1g_{9/2}$	0.19	.94	.32
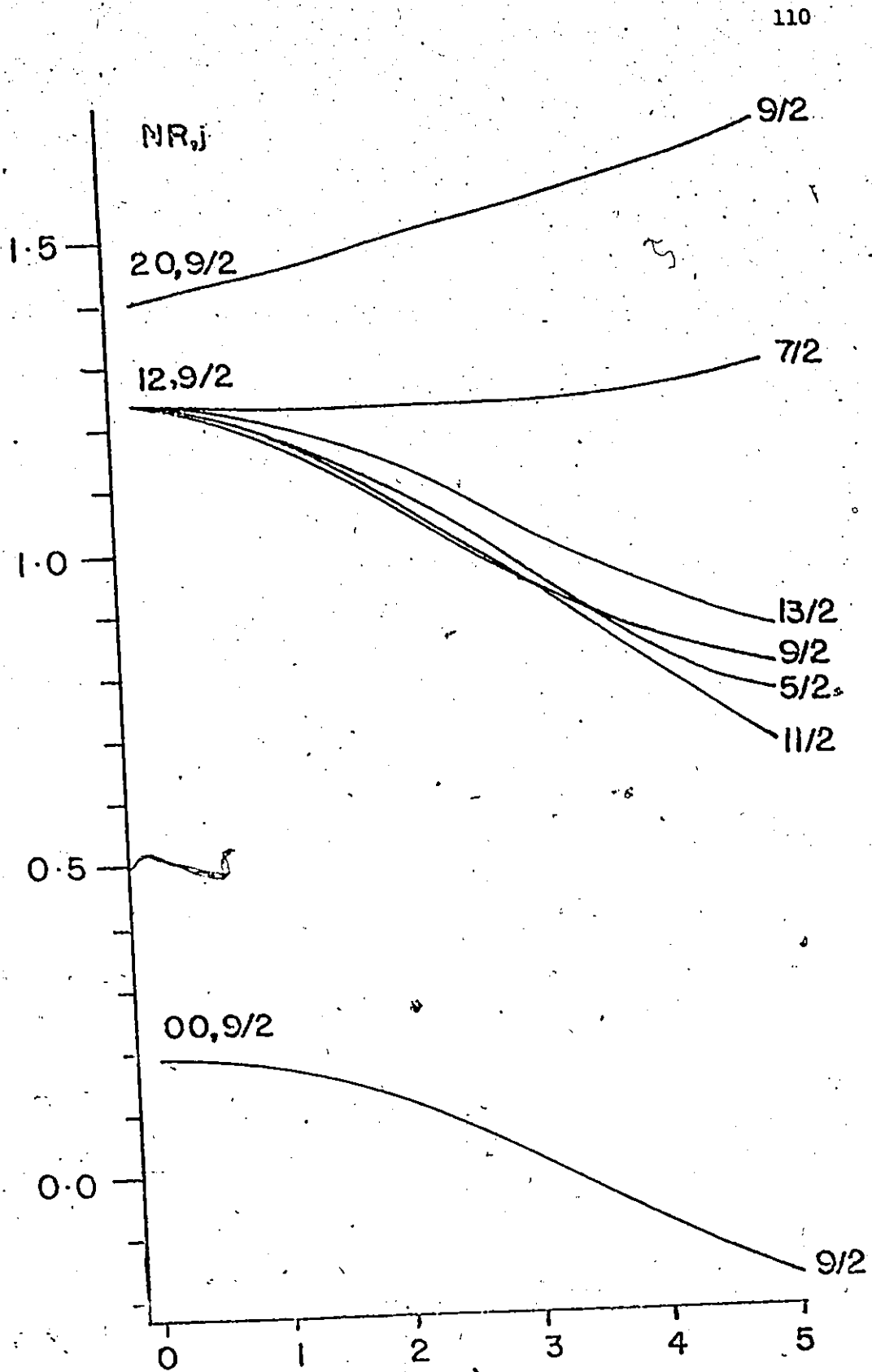
Figure 5.4

A comparison between the experimental level scheme of ^{71}Ge and that predicted by the intermediate-coupling model, with the core and quasi-particle parameters as given in figures 5.2 and 5.3, and with the coupling parameter $\xi = 4$.
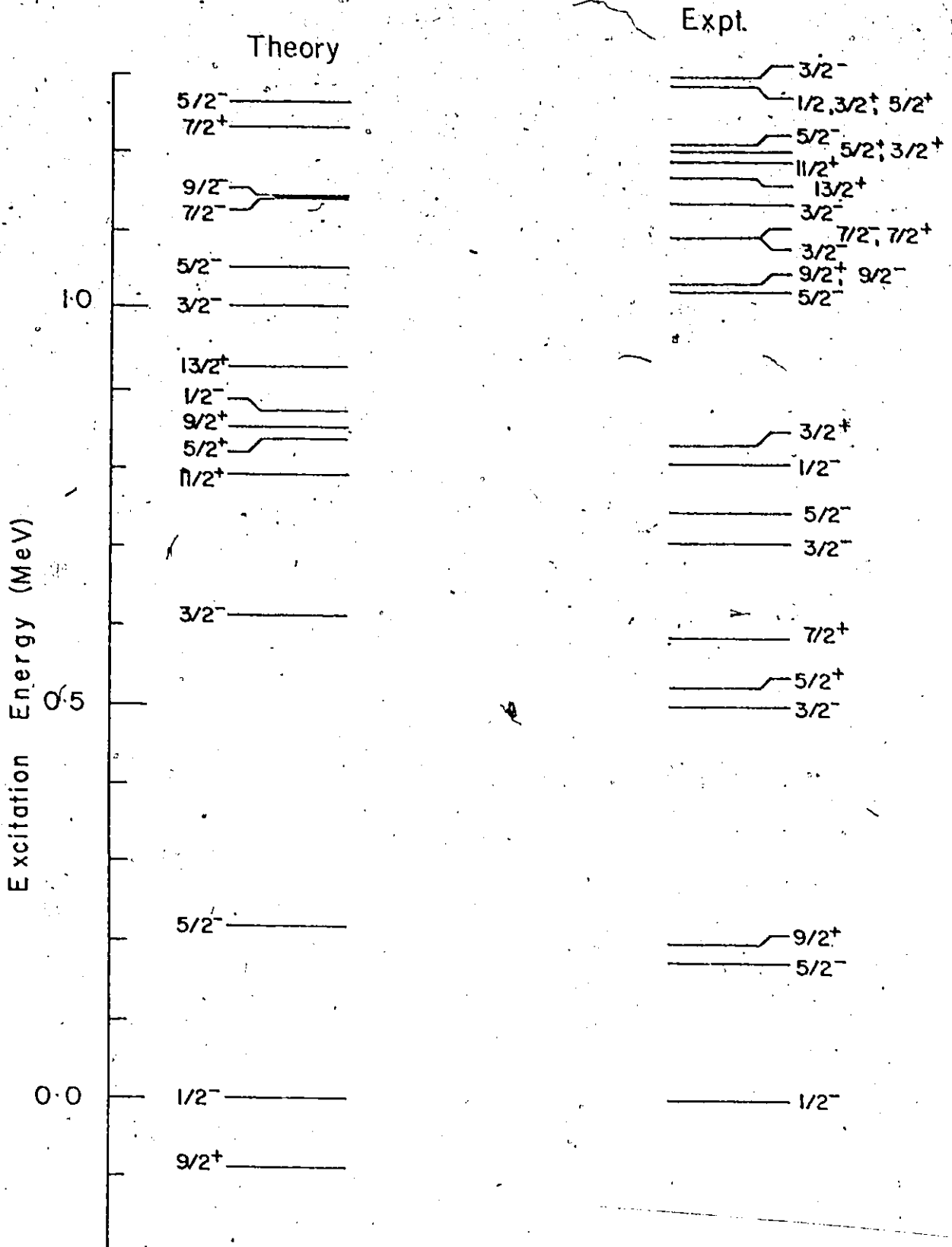
CHAPTER 6

SUMMARY AND CONCLUSIONS

The $^{68}Zn(\alpha,n\gamma)^{71}Ge$ reaction has proved to be a useful tool in the study of the excited states of ^{71}Ge. The angular momenta of most of the levels in ^{71}Ge below 1.3 MeV excitation energy have been determined by measuring gamma-ray angular distributions, and angular correlations of gamma-gamma cascades, using the Compound Nucleus Statistical Model to describe the (α,n) reaction.

A nuclear model calculation of ^{71}Ge, assuming that the odd neutron in ^{71}Ge is coupled to collective quadrupole vibrations of the ^{70}Ge core, including corrections for a pairing residual interaction between the core nucleons, has limited success in reproducing the level structure of ^{71}Ge. The inadequacies of the theory are particularly evident in predicting the positions of the lower-lying positive parity levels.

Scholz and Malik (1968) have had some success in explaining properties of the odd-neutron nuclei Ga, As, Br, and Rb, by assuming that these nuclei have a permanent prolate deformation. The rotational band structure expected in the level schemes of deformed nuclei is obscured by strong coupling between the rotational motion and quasi-particle

excitations. This Coriolis-coupling model has been applied to the positive-parity levels in the odd-neutron nucleus ^{75}Se (Sanderson, 1973), to explain the existance of a low-lying $5/2^+$ level and $7/2^+$ level. It appears that such a model might pro-vide a better first approximation to the level structure of ^{71}Ge, than the intermediate-coupling model described in Chapter 5.

excitations. This Coriolis-coupling model has been applied to the positive-parity levels in the odd-neutron nucleus ^{75}Se (Sanderson, 1973), to explain the existance of a low-lying $5/2^+$ level and $7/2^+$ level. It appears that such a model might pro-vide a better first approximation to the level structure of ^{71}Ge, than the intermediate-coupling model described in Chapter 5.

BIBLIOGRAPHY

Alvar, K.R. (1973). Nuclear Data Sheets 10, 205.

Bardeen, J., Cooper, L.N. and Schrieffer, J.R. (1957).
        Phys. Rev. 108, 1175.

Birstein, L., Chechik, R., Drory, Ch., Friedman, E., Jaffe A.A.
        and Wolf, A. (1968). Nucl. Phys. A113, 193.

Bohr, A. (1952), K. Danske Vidensk. Selsk. Mat.-Fys. Medd.
        26, No. 14.

Bohr, A. and Mottelson, B.R. (1953). K. Danske Vidensk. Selsk.
        Mat.-Fys. Medd. 27, No. 16.

Bohr, A., Mottelson, B.R. and Pines, D., (1958). Phys. Rev 110,
        936.

Bjorkland, F. and Fernbach (1958). Phys. Rev. 109, 1296.

Camp, D.C. (1968). Nucl. Phys. A121, 561.

Camp, D.C. Fielder, D.R. and Foster, B.P.(1971).
        Nucl. Phys. A163, 145.

Camp, D.C. and Foster, B.P. (1971). Nucl. Phys. A177, 401.

Camp, D.C. and Van Lehn, A.L. (1969). Nucl. Instr. and Meth.
        76, 192.

Castel, B., Stewart, K.W.C. and Harvey, M. (1971). Nucl. Phys.
        A162, 273.

Choudhury, D.C. (1954). K. Danske Vidensk. Selsk. Mat.-Fys.
        Medd. 28, No. 4.

Choudhury, D.C. and O'Dwyer, T.F. (1967). Nucl. Phys. A93,
        300.

Ericson, T., (1963) Annals of Physics 23, 390.

Ericson T. and Mayer-Kuckuk, T. (1966). Annual Reviews of
        Nuclear Science 16, 183.

Ferguson, A.J. (1965). Angular Correlation Methods in
        Gamma-Ray Spectroscopy. (North-Holland Publ. Co.,
        Amsterdam).

Forsston, K., Hasselgren, A., Monseu, Ph., Nilsson, A. and
        Sawa, Z.P. (1974). Physica Scripta 10, 51.

Fournier, R., Kroon J., Hsu, T.H. and Hird, B. (1973).
Nucl. Phys. A202, 1.

Goldman, L.H. (1968) Phys. Rev. 165, 1203.

Glendenning, N.K., (1960). Phys. Rev. 119, 213.

Green, P.W. (1971). University of Alberta Internal Report.
UAE-NPL-27, unpublished.

Hecht, K.T. (1964). Selected Topics in Nuclear Spectroscopy.
Ed. Verhaar, B.J. (North-Holland Publ. Co., Amsterdam).

Heyde K. and Brussard, P.J. (1967). Nucl. Phys. A104, 81.

Hinrichsen, P.F., Van Patter, D.M. and Shapiro, M.H. (1969).
Nucl. Phys. A123 250.

Hsu, T.H., Fournier, R., Hird, B. and Kroon, J. (1972).
Nucl. Phys. A179, 80.

Janes, A.N., Twin, P.J. and Butler, P.A. (1974). Nucl. Instr.
and Meth. 115, 105.

Kisslinger, L.S., and Sorensen, R.A. (1963). Rev. Mod. Phys.
35, 853.

Kregar, M. and Mihailovic M.V. (1967). Nucl. Phys. A93, 402.

Malan, J.G., Tepel, J.W., and de Villiers, J.A.M. (1970).
Nucl. Phys. A143, 53.

Malan, J.G., Barnard E., de Villiers, J.A.M. and Van der Merwe, P.
(1974) Nucl. Phys. A227, 399.

Murray, G., Sanderson, N.E., and Willmott J.C. (1971).
Nucl. Phys. A171, 435.

Nilsson, S.G. (1955). K. Danske Vidensk. Selsk. Mat.-Fys.
Medd. 29, No. 16.

Onizuka, Y., Sugimitsu, T., Kato, N. and Kuroyanagi, T. (1975).
J. Phys. Soc. Japan 38, 308.

Perey, C.M. and Perey, F.G. (1974). Atomic Data and Nuclear
Data Tables 13, 293.

Rose, H.J. and Brink, D.M. (1967). Rev. Mod. Phys. 39, 306.

Rustgi, M.L., Lucas, J.G. and Mukherjee, S.N., (1968). Nucl. Phys. A117, 321.

Sanderson, N.E. (1973). Nucl. Phys. A216, 173.

deShalit, A. and Talmi, I. (1963). Nuclear Shell Theory. (Academic Press, New York).

Sheldon, E. and Van Patter, D.M. (1966). Rev. Mod. Phys. 38, 143.

Sheldon, E. and Strang, R.M. (1969). Computer Physics Communications 1, 35.

Scholz, W. and Malik, F.B. (1968). Phys. Rev. 176, 1355.

Simpson, J.J., Smilansky, U. and Ashery D. (1969). Nucl. Phys. A138, 529.

Simpson, J.J., Ward, D. and Ewan, G.T. (1972). Nucl. Phys. A135, 553.

Temmer, G.M. and Heydenburg, N.P. (1956). Phys. Rev. 104, 967.

Thankappen, V.K. and True, W.W. (1965). Phys. Rev. 137, B793.

Van Hise, J.R. and Rainis, A.E. (1972). Phys. Rev. C6, 164.

Vogt, E. (1968). Advances in Nuclear Physics 1, 261. (Plenum Press, New York).

Weishaupt, R. and Robenstein, D. (1972). Z. Physik 251, 105.

APPENDIX A

DATA ACQUISITION SYSTEM

A-1   A Description of the Hardware

The computer-based data acquisition system at the
McMaster University Accelerator Laboratory is based on a
PDP-9* processor, with a core memory of 8K (1K = 1024) words
of 18 bits each.   It is interfaced to a peripheral memory
of 32K 18 bit words, which can be used to store data, but
cannot hold programs to be executed.

Standard peripherals supplied by the computer
manufacturer consist of two DEC-tape drives, a teletype, a
paper reader/punch, an IBM compatible 7-track magnetic tape
drive, and a cathode ray display screen with a 'Scan-master'
controller.   Other devices which have been interfaced locally
are (1) a set of push-buttons that can be sensed by the
computer, (2) a set of light-emitting diode numeric display
registers (3) a set of 12 scalers for counting pulses,
(4) a controller for analogue to digital converters (McNaught,
1974), and (5) an incremental plotter.

The ADC interface can control up to 8 ADC's, and can
operate in 'singles' mode, where each ADC presents data to
the computer independently of the others; and in 'coincidence'

---

*Manufactured by Digital Equipment Corp., Maynard, Mass., U.S.A.

mode, where a group of ADC's are read every time the interface signals to the computer that data have been digitised.

A-2 Singles Programs

A common requirement of a nuclear experiment is a device to accumulate pulse height spectra, or histograms of number of events as a function of pulse height, from signals from one or more independent detectors. The high resolution of Ge(Li) detectors frequently requires that the data collection device should have a resolution of one part in a few thousand in measuring and storing the pulse height information, so that useful information is not lost. Count rates of greater than 10^4 events per second per detector are not uncommon. Programs have been written for the PDP-9 computer to accumulate spectra from such data.

The programs are written in assembler language, because of the relatively small size of the programmable memory, and are self-contained, i.e. they use none of the so-called "system device handlers" or subroutines supplied by the computer manufacturer to facilitate input and output. The main objectives in writing the programs have been to make them easy to use, relatively flexible, and easy to extend to provide new functions when required. The minimal requirements of such an on-line computer are that it should gather spectra on command; display these spectra to the experimenter, so that the progress of the experiment can be monitored; write

out the spectra in some permanent form for later analysis,
and allow some analysis to be carried out during the course
of the experiment.

Communications from the experimenter to the computer
are made through the teletype or the push-buttons. The tele-
type commands have a simple form, one or two letters (having
some mnemonic value) followed by a string of integers,
separated by commas, to be used as parameters in the command.

Data can be taken from one to eight ADC's (as long as
the total memory required for data storage is less then 32K),
and each ADC can collect a spectrum of up to 8K channels. The
memory space allotted to each ADC is assigned by teletype
command after the program has been loaded, and can easily be
changed at any time. Commands are available to instruct the
computer on which ADC's and scalers are to be used; to initiate
collection of data; and to stop collection. Data can be
gathered for a pre-set time interval; for a preset number of
pulses in one of the scalers; or until a command from the
teletype is given. The ADC's are handled under program
control i.e. when an ADC has digitised a pulse the ADC
controller interrupts the computer from its foreground task
(of displaying data, etc); the computer ascertains that the
ADC was the device which caused the interrupt, and reads a
word from the ADC controller. The bottom 13 bits of the
ADC word contain the actual pulse height information, the
next 3 bits contain the number of the ADC which caused the

interrupt. The computer uses the ADC number as the index
of a list of starting locations of the region of memory
allotted to the spectrum of each ADC, and adds the relevant
start location to the pulse height number to find the location
in memory to increment. This mode of operation gives
flexibility in assigning different memory regions to the
ADC's, but suffers from the disadvantage that significant
losses of data can occur at high count rates because of the
time taken to process each event (about 40 μ sec). Changes
in the ADC controller are anticipated, which will allow the
relevant memory locations to be incremented directly by
hardware, and decrease the losses.

While waiting for a teletype command the computer
displays one of the collected spectra on the cathode-ray
display, and the channel number and channel contents of a
channel selected and intensified by the scan-master controller'
are displayed in two of the light-emitting-diode numeric
displays.

Spectra are stored in a relatively permanent form
on DEC-tapes, which are small magnetic tapes widely used by
Digital Equipment Corp. These tapes have a block-addressable
structure; one DEC-tape reel normally contains 576 blocks of
256 18 bit words. Each block is numbered, and the computer
can access any block for reading or writing. A simple compact
format for storage of data has been adopted, in which the
first block on the tape is used as a directory containing the

starting block number, and length of each spectrum which has been written on the tape. The directory information is updated automatically each time a spectrum is written onto tape.

Spectra can be plotted on an incremental plotter, with axes, without significantly affecting the collection of data.

Commands for manipulation of spectra exist. It is possible to smooth spectra, by performing a weighted moving three-point average over channel contents, or add or subtract different spectra. A limited amount of analysis of the spectra can be performed, by summing the numbers of counts in selected regions of a spectrum. More extensive analysis features are planned.

A-3 Multiparameter Programs

In a coincidence experiment, generally more than one parameter must be recorded each time an event occurs. For example, in a gamma-gamma coincidence experiment every time an event of interest occurs, it is necessary to record the energies of the two gamma rays and the difference in their arrival times in the detectors. Typically the gamma-ray energy pulses are digitised by ADC's with conversion gains of 4K channels. One method of storing the incoming information (neglecting the time signal) would be to build up an array of dimensions 4096 by 4096, but this would require a randomly-

accessible memory with more than 16 x 10⁶ locations. A magnetic core memory of this size is expensive. A financially more attractive method of dealing with the data storage problem, which can readily be extended to include more than two parameters, has been implemented using the PDP-9 computer and the IBM compatible magnetic tape unit. The pairs (or multiplets) of ADC words are stored in sequential fashion on magnetic tape in the order that they arrive. To make efficient use of the magnetic tape and to average out statistical fluctuations in the incoming data rate, the data are accumulated in a list in a buffer in the memory of the computer, until the buffer is full; the incoming data are then automatically routed into a second buffer while the first is written onto tape. When the second buffer is full, it is written out while the first is re-filled. It is possible to accumulate data at the rate of some hundreds of events per second before the tape writing speed limits the data acquisition speed.

The ADC interface on the PDP-9 computer was designed so that up to 7 ADC's could be used in coincidence mode, while the eighth can run independently of the others. When one of the coincidence ADC's receives a pulse, the ADC controller waits for a period of time (generally set to 4 microseconds) to allow the other ADC's to receive their pulses, then turns off the inputs to all the other coincidence ADC's. When all the ADC's have digitised their pulses the computer is interrupted. After recognising the interrupt, the computer reads data from all the enabled coincidence ADC's,

and stores the ADC words in a buffer. If the buffer has
room for more data the computer reverts to its normal fore-
ground task of displaying spectra, but if the buffer is full
the computer sets a software flag and re-arranges pointers
within the program to route successive data into a second
buffer; then returns to the display loop. In this display
loop the computer repetitively checks the buffer-full soft-
ware flag, and when this is found to be set, the program
leaves the loop to update spectra of each active ADC, from
the full buffer, and writes the buffer onto magnetic tape.

The block, or physical record, size on tape is 512
words, this being a compromise between efficiency of packing
the data onto tape (implying a long record) and use of the
computer core (which is required for the program) for buffer
space. On each record on tape the first word is a run
number, which is set by the experimenter to identify data
taken during a particular part of an experiment; the second
word is a record number which is incremented by one each time
a buffer is written. A buffer can be written in about $\frac{1}{2}$ sec.,
so with 2 parameter data about 500 events per second can be
logged.

The commands to the event-by-event multiparameter
programs are similar to those of the singles programs, allow-
ing spectra to be written out on DEC-tape, plotted, and
manipulated, with additional commands to control the magnetic
tape.

APPENDIX B

DATA RECOVERY SYSTEM

Appendix A-3 described how multiparameter data can be
stored on magnetic tape in event-by-event mode. To extract
useful information from the experiment it is necessary to
compress the data to a manageable form. Considering the
example of a gamma-gamma coincidence experiment, the raw data
consist of pairs of words on tape representing the energies of
the two gamma rays. One requires to set digital windows on
peaks which appear in the spectrum of all the events in one
detector (the projected spectrum) and scan through the tapes,
presumably with a computer, picking out those events in
which one gamma-ray energy is within a selected window range,
building up separate spectra of the other gamma energy for
each digital window. To reduce the time spent in scanning
the tapes it is desirable to build up as many gamma spectra
as possible per pass of the tape. A computer with a large
amount of core memory could be used for tape scanning, but
an alternative solution uses a small computer with a disk for
storage of the accumulated spectra.

The PDP-15 computer at the McMaster University Tandem
Lab has 16K of fast core, and a fixed-head disk capable of
storing 256K of 18 bit words. Thus the disk is capable of

holding up to 64 4K spectra. The PDP-15 disk is relatively well suited for use as a random-access device because of its ability to read or write single words on the disk; most disks read or write blocks of words, of some minimum length. A problem arises with the use of the disk because of its relatively slow random access time for individual words. Typically a word representing a channel content can be read from core memory, updated, and re-written in at most a few microseconds, whereas the average time to read and re-write a single word on the disk is the time required for the disk to go through $1\frac{1}{2}$ revolutions, i.e. 25×10^{-3} secs. Thus if the disk were used directly as a random access device, only about 40 events per second could be processed. The average update rate on the disk can be increased by buffering and de-randomising the events to go on the disk, so that many words are updated per two revolutions of the disk.

A routine, partially based on a program written by D. Sinclair, written in assembler language, callable from a FORTRAN program, using buffering techniques to achieve update rates of 600 events per second, has been implemented on the PDP-15 computer. The use of FORTRAN as the control program encourages flexibility in writing programs to analyse different types of coincidence data. The disk-update procedure is partially overlapped with computation in the calling FORTRAN program, so that the disk-updating time does not necessarily add significantly to the time required by the

FORTRAN program to read raw data from magnetic tape and to check window lists etc.

Reference:

McNaught, R.A. (1974), Digital Equipment Users Society, Seventh Canadian Symposium Proceedings, 81.